



**To my beloved family...**

**Për familjen time të dashur...**

**DECIPHERING IKBKE INVOLVEMENT  
IN  
HEPATOCELLULAR CANCER HEPG2 CELLS**

A THESIS SUBMITTED TO  
THE GRADUATE SCHOOL OF ENGINEERING AND SCIENCE  
OF BILKENT UNIVERSITY  
IN PARTIAL FULFILLMENT OF THE REQUIREMENTS FOR  
THE DEGREE OF MASTER OF SCIENCE  
IN  
MOLECULAR BIOLOGY AND GENETICS

By  
Erta Xhafa  
June 2020

## **Deciphering IKBKE involvement in hepatocellular cancer HepG2 cells**

By Erta Xhafa

June 2020

We certify that we have read this thesis and that in our opinion it is fully adequate, in scope and in quality, as a thesis for the degree of Master of Science.

---

Serkan İsmail Göktuna (Advisor)

---

Onur Çizmeciöđlu

---

Mesut Muyan

Approved for the Graduate School of Engineering and Science:

---

Ezhan Karařan

Director of the Graduate School of Engineering and Science

## Abstract

### DECIPHERING IKBKE INVOLVEMENT IN HEPATOCELLULAR CANCER HEPG2 CELLS

Erta Xhafa

M.S. in Molecular Biology and Genetics

Advisor: Serkan İsmail Göktna

June, 2020

Hepatocellular carcinoma (HCC) is the second leading cause of cancer related deaths worldwide. The reasons behind high mortality in HCC patients include late diagnosis and lack of therapeutic option. Sorafenib is the only FDA approved systemic therapy for advanced HCC patients but it improves patients' survival with only 4 months. For this reason, better understanding of the mechanisms of tumor initiation, development and drug resistance in HCC would create new treatment opportunities for HCC patients. In this study, the role of IKK $\epsilon$  in HCC tumorigenesis is analysed. HCC development is tightly related to inflammation and IKK $\epsilon$  is an inflammation related kinase with very well-known roles in regulating NF- $\kappa$ b and interferon signalling upon viral infection. However, it has also been linked to tumorigenesis of multiple cancers including breast cancer, pancreatic cancer and ovarian cancer. Loss of function models via shRNA or CRISPR/Cas9 are used to study the role of IKK $\epsilon$  in HCC tumorigenesis. Depletion of IKK $\epsilon$  in HepG2 cells improves the proliferation and anchorage-independent growth of the cells *in vitro* and it induces a decrease in the expression of EMT markers. Similarly, IKK $\epsilon$  depleted HepG2 cells withstand higher doses of Sorafenib, hence, supporting a tumor suppressive potential of IKK $\epsilon$  in tumor initiation stages. However, IKK $\epsilon$  appears to be involved in EMT and upregulated in EGF and TGF $\beta$ 1 signalling, two important signalling inducing EMT in HepG2 cells. IKK $\epsilon$  is also shown to be upregulated in Sorafenib resistant HepG2 cells where its pharmacological inhibition sensitized Sorafenib resistant HepG2 cells to Sorafenib.

These findings show an oncogenic potential of IKK $\epsilon$  in later stages of tumor development including metastasis and drug resistance. The results presented in this study suggest a dual role of IKK $\epsilon$  in HCC development and drug resistance. Therefore, further mechanistic analysis on this involvement could reveal IKK $\epsilon$  inhibition as a potential therapeutic strategy for overcoming Sorafenib resistance in HCC patients.

Key words: HCC, IKK $\epsilon$ , EMT, drug resistance.

## Özet

# HEPATOSELÜLER KANSER HEPG2 HÜCRELERİNDE IKKε'NİN NASIL YER ALDIĞININ ÇÖZÜMLENMESİ

Erta Xhafa

Moleküler Biyoloji ve Genetik Yüksek Lisansı

Tez Danışmanı: Serkan İsmail Göktuna

Haziran, 2020

Hepatoselüler karsinom (HSK/HCC), dünya çapında kansere bağlı ölümlerin önde gelen ikinci nedenidir. Hepatoselüler karsinom hastalarındaki yüksek ölüm oranının altında yatan nedenler arasında geç tanı konulması ve yeterli terapötik seçeneklerin olmaması yer almaktadır. Sorafenib, ileri derece HCC hastaları için FDA tarafından onaylanmış tek sistemik terapi olmasına karşın hastaların yaşam süresini sadece 4 ay kadar uzatabilmektedir. Bu nedenle HCC'de tümör başlangıcı, gelişimi ve ilaç direnci mekanizmalarının daha iyi anlaşılması, HCC hastaları için yeni tedavi olanaklarının sunulması açısından büyük önem arz etmektedir. Bu çalışmada, IKKε'un HCC tümör oluşumundaki rolü incelenmiştir. HCC gelişiminin inflamasyon ile yakından ilişkili olmasının yanında IKKε, viral enfeksiyon durumunda interferon sinyal yolağının ve NF-κb'nin regülasyonunda rol oynayan inflamasyon ilişkili kinaz olarak bilinmektedir. Ek olarak meme kanseri, pankreas kanseri ve yumurtalık kanseri gibi pek çok kanserde, tümör oluşumunun başlaması ile ilişkilidir. Fonksiyon kaybı modelleri shRNA ya da CRISPR/Cas9 yöntemleri ile oluşturulmuş olup bu modeller kullanılarak IKKε'un HCC tümör oluşumu başlangıcındaki rolleri çalışılmıştır. HepG2 hücrelerinde IKKε delesyonu, hücrelerin in vitro proliferasyonlarını ve yüzey-bağımsız büyümelerini arttırmakta ve EMG (epitel-mezenkimal geçiş) belirteçlerinin ekspresyon seviyesinde düşüşe neden olmaktadır. Aynı doğrultuda; IKKε delesyonu gerçekleştirilen HepG2 hücreleri, Sorafenib'in yüksek dozlarına karşı direnç

göstermekte ve buna bağı olarak IKKε'un tümör başlangıç aşamalarındaki tümör baskılayıcı potansiyelinin bu sayede arttığı görülmektedir. Fakat, IKKε'un EMG'de rol aldığı ve HepG2 hücrelerinde EMG'yi indükleyen iki önemli sinyal yolağı olan EGF ve TGFβ1 sinyal yolağında yukarı doğru düzenlendiğı diğere bir deyişle ekspresyon seviyesi artmış durumda olduğı görülmektedir. Buna ek olarak; farmakolojik inhibisyon ile Sorafenib'e karşı dirençli olan HepG2 hücrelerinin Sorafenib'e duyarlı hale getirilmesi üzerine bu hücrelerde de IKKε'un yukarı doğru düzenlendiğı gösterilmiştir. Bu bulgular, metastaz ve ilaç direnci gibi tümör gelişiminin ileri aşamalarında IKKε'un onkojenik potansiyelini göstermiştir. Dolayısıyla bu mekanizmayı anlamaya yönelik ileri analizler, HCC hastalarında Sorafenib direncinin üstesinden gelebilmek için IKKε inhibisyonunun yeni bir terapötik strateji olarak sunulması yolunda yeni olanaklar yaratabilme kapasitesine sahiptir.

Anahtar kelimeler: HSK, IKKε, EMG, ilaç dirençliliğı.

## Acknowledgements

I would like to express my very great appreciation to my advisor Assist. Prof. Serkan İsmail Göktuna for his supervision throughout my graduate studies and trusting me with the projects. I have gained immense knowledge and experience all thanks to his guidance, support and feedback and I will always be grateful.

I am deeply in debt to Dr. Tieu Lan Chau for sharing all her expertise in the field with me. Her instructions, advices and support have been absolutely beneficial to me and to the finalization of this Master thesis and I will always be grateful.

I would like to express my deepest appreciation to my former professors and committee members: Assist. Prof. Onur Çizmecioğlu and Prof. Mesut Muyan for their intellectual guidance throughout my studies and in completion of this thesis.

I would like to acknowledge all the faculty, staff and members of the MBG Department in Bilkent University. They have made my graduate studies valuable, easier and unforgettable.

I owe my deepest gratitude to my family for the unconditional love. Nothing would have been possible without their full trust in my choices. They have been my daily inspiration.

I am grateful to the unconditional support, love and patience that my Suard has given to me, motivating and encouraging me in the most difficult days.

Lastly, I thank TÜBİTAK (117Z277) for funding this research study and Bilkent University for supporting my graduate study.

## Table of content

Approval Page.....	ii
Abstract.....	iii
Özet .....	v
Acknowledgements .....	vii
Table of content .....	viii
List of Figures .....	xi
List of Tables .....	xii
CHAPTER 1: Introduction .....	1
1.1. Hepatocellular carcinoma .....	1
1.1.1. Molecular events in HCC .....	2
1.1.2. Surveillance, diagnosis, staging system and therapeutic options for HCC	
1.1.1. Molecular events in HCC .....	4
1.1.3. Systemic therapy for advanced HCC patients .....	5
1.1.4. Mechanisms of sorafenib resistance .....	6
1.2. IKBKE gene .....	7
1.2.1. The role of IKBKE in innate immunity response .....	7
1.2.2. The role of IKBKE in oncogenesis .....	9
1.2.2.1. IKBKE expression levels in different cancers.....	9
1.3. IKBKE's association with different pathways in cancer .....	11
1.3.1. IKBKE and NF- $\kappa$ B .....	11
1.3.2. IKBKE and PI3K/AKT .....	12
1.3.3. IKBKE and HIPPO signalling pathway .....	13
1.3.4. IKBKE and other pathways .....	13
CHAPTER 2: Materials and Methods .....	15
2.1. Materials .....	15
2.1.1. Chemical and reagents .....	15

2.1.2. Kits .....	16
2.1.3. Cell culture components .....	17
2.1.4. Buffers .....	19
2.1.5. Antibodies .....	20
2.1.6. Primers .....	22
2.2. Methods .....	24
2.2.1. Cell lines, cell culture and reagents .....	24
2.2.2. Cryopreservation .....	24
2.2.3. Recovery of cryopreserved cells .....	24
2.2.4. Cell maintenance and propagation .....	25
2.2.5. Lentiviral shRNA/CRISPR-Cas9 transfection/ transduction .....	25
2.2.6. IKK $\epsilon$ overexpression .....	26
2.2.7. CellTiter-Glo Luminescent cell viability assay .....	26
2.2.8. Cell Proliferation Reagent WST-1 .....	27
2.2.9. Real Time Cell Analysis (RTCA) – Proliferation .....	27
2.2.10. Colony Formation Assay .....	27
2.2.11. Anchorage independent growth assay .....	27
2.2.12. Cell cycle analysis through Propidium Iodide staining .....	28
2.2.13. Wound healing assay .....	28
2.2.14. Western Blotting .....	28
2.2.15. Real-Time PCR .....	29
CHAPTER 3: Results .....	30
3.1. HepG2 cell proliferation negatively correlates to IKK $\epsilon$ expression. ....	30
3.2. HepG2 cells show more anchorage independence growth upon IKK $\epsilon$ depletion .....	30
3.3. EMT status of HepG2 cells shifts upon depletion or ectopic expression of IKK $\epsilon$ . .....	33

3.4. TGFβ1 induced proliferation in HepG2 cells is dependent on IKKε expression .....	35
3.5. IKKε is involved in TGFβ1 signalling through AKT activation .....	36
3.6. EGF signalling in HepG2 cells activates IKKε .....	37
3.7. Sorafenib resistance of HepG2 cells improves upon IKKε depletion or pharmacological inhibition .....	38
3.8. Preparation of HepG2 Sorafenib resistant cell lines .....	38
3.9. Sorafenib resistance of HepG2 SORA/B cells reduces upon pharmacological inhibition of IKKε .....	44
CHAPTER 4: Discussion .....	46
CHAPTER 5: Conclusion and Future Perspective .....	51
Bibliography .....	53

## List of Figures:

Figure 1.1: Estimated worldwide incidences and mortality of top 10 cancer types ...	1
Figure 1.2: Molecular alterations contributing to HCC development .....	2
Figure 1.3: BCLC staging system for HCC patients .....	5
Figure 3.1: HepG2 cell proliferation negatively correlates to IKK $\epsilon$ expression. ....	31
Figure 3.2: HepG2 cells show more anchorage independence upon IKK $\epsilon$ depletion .....	32
Figure 3.3: EMT status of HepG2 cells is altered upon IKK $\epsilon$ depletion .....	33
Figure 3.4: Ectopic expression of IKK $\epsilon$ in HepG2 cells induces EMT shift .....	34
Figure 3.5: TGF $\beta$ 1 induced proliferation in HepG2 cells is dependent on IKK $\epsilon$ expression .....	35
Figure 3.6: IKK $\epsilon$ is involved in TGF $\beta$ 1 signalling through AKT activation.....	37
Figure 3.7: EGFR signalling in HepG2 cells activates and upregulates IKK $\epsilon$ .....	38
Figure 3.8: Resistance of HepG2 cells to Sorafenib treatment improves upon IKK $\epsilon$ depletion or pharmacological inhibition .....	39
Figure 3.9: Schematic representation of Sorafenib resistant HepG2 cell line development .....	40
Figure 3.10: Sorafenib IC <sub>50</sub> of HepG2 SOR cells .....	41
Figure 3.11: Stability of Sorafenib IC <sub>50</sub> of HepG2 SORB9 cells upon removal of Sorafenib from culture medium .....	42
Figure 3.12: Morphology and expression of EMT markers in HepG2 SOR cells ....	43
Figure 3.13: IKK $\epsilon$ is important for the survival of Sorafenib resistant HepG2 cells .....	45

## List of Tables:

Table 2.1. Chemicals and reagents used in this study .....	15
Table 2.2. Kits used in this study .....	16
Table 2.3. Cell culture media, chemicals and reagents used in the study .....	17
Table 2.4. Buffers and their compositions .....	19
Table 2.5. Antibodies used in this study .....	21
Table 2.6. Primers used in this study .....	23
Table 2.7. Components for calcium phosphate transfection and their amounts .....	26
Table 2.8. List of plasmids used in lentiviral transfection .....	26
Table 2.9. Components in RT-PCR mixture .....	29

# CHAPTER 1

## Introduction

### 1.1. Hepatocellular carcinoma

Liver cancer is ranked sixth as the most common diagnosed cancer with over 800,000 new cases only in 2018 alone. Additionally, it is the third cause of cancer-related deaths with a significantly high mortality rate (Figure 1.1) [1]. Reasons behind the high mortality rate in liver cancer patients include late diagnosis and lack of therapeutic options [1]. Liver cancer incidences and mortality show geographical heterogeneity with significantly more cancer cases in developing and under-developed countries [1]. Moreover, liver cancer occurs more often in males than in females with a ratio 3:1 despite the geographical location [1].

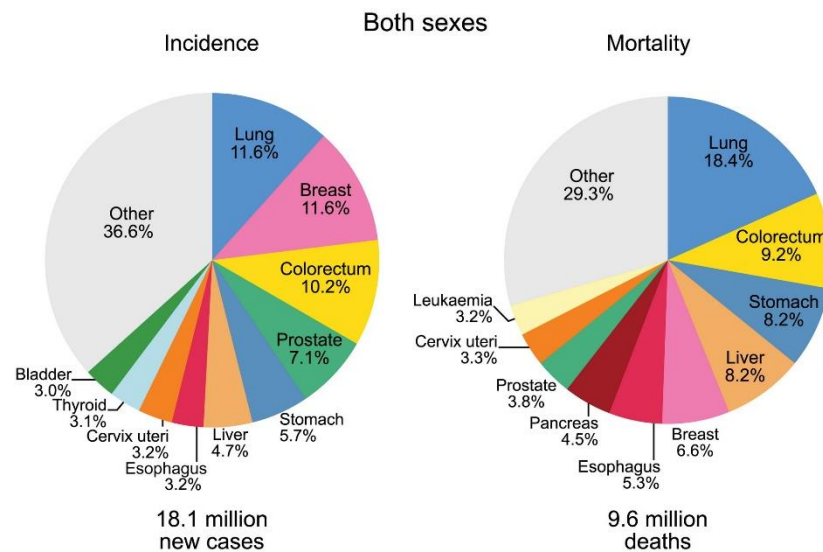


**Figure 1.1:** Estimated worldwide incidences and mortality of top 10 cancer types. Reproduced with permission from John Wiley & Sons, Inc. [1]

Hepatocellular carcinoma (HCC) is the primary liver cancer representing 85-90% of all liver cancer cases [2]. The main risk factors contributing to HCC development are chronic liver disease, chronic inflammation with hepatitis B or/and C (HBV, HCV), and cirrhosis [2]. Other risk factors include alcoholic liver disease, non-alcoholic fatty

liver disease, metabolic disorders, toxins and other genetic conditions [2]. Majority of these risk factors lead to cirrhosis, present in more than 80% of HCC patients, and ultimately HCC [2]. Moreover, the risk factors contribute to a nonresolving inflammation in liver where macrophages and other immune cells get infiltrated, cytokine production is dysregulated and the wound-healing response perpetuates causing fibrosis, cirrhosis and HCC. Hence, HCC is considered an inflammation-associated cancer where the inflammation in the microenvironment plays a pivotal role in disease progression.

### 1.1.1. Molecular events in HCC

HCC develops in a multistep process. In most of the cases, it arises upon chronic liver damage, fibrosis and cirrhosis. Pre-cancerous nodules develop in cirrhotic livers and are known as low-grade dysplastic nodules (LGDNs) [3]. They advance into high-grade dysplastic nodules (HGDNs) which further progress into early stage HCC and latter advanced HCC (Figure 1.2.) [3]. As malignant transformation into HCC progresses, multiple genetic alternations accumulate inside a cancerous cell that affect aspects such as proliferation, invasion and metastasis. Very frequently, in different nodules of the same liver, more than 40 different somatic alternations can accumulate which can be a mixture of both genetic alternations and epigenetic modifications that can directly affect gene expression levels of tumor suppressors and oncogenes [3]. Hence, HCC is a very complex and heterogenous neoplasia where dysregulation of multiple pathways contributes to initiation, development and progression of the disease.

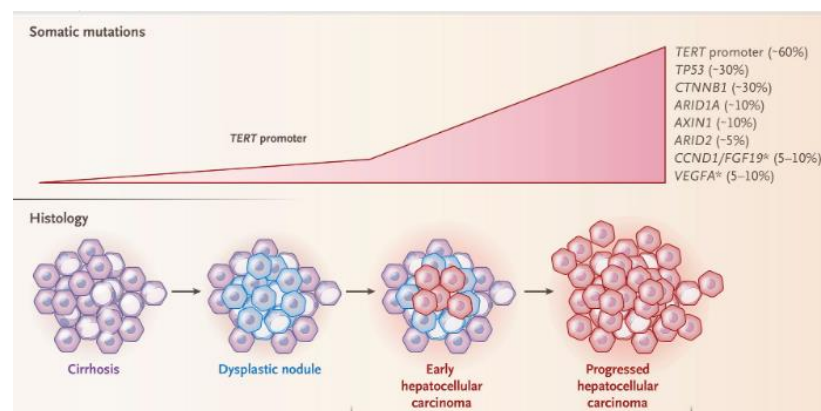


**Figure 1.2:** Molecular alterations contributing to HCC development. Reproduced with permission from Villanueva, 2019, Copyright Massachusetts Medical Society.

Frequently observed dysregulated signalling pathways that contribute to progression of nodules from LGDN to HGDN and finally HCC are WNT signalling, protein-folding machinery, expression of fetal genes and re-expression of telomerase enzyme due to mutations in TERT promoter [3]. Telomerase is not normally expressed in hepatocytes but its re-expression contributes to uncontrolled proliferation of hepatocytes in cirrhotic or non-cirrhotic liver and it is selected during malignant transformation. TERT promoter mutations are seen in more than 90% of HCC cases [3]. The most important promoters of HCC are HBV and HCV chronic infection. 80% of HCC cases occur in patients infected with HBV and 75% of patients infected with HCV develop HCC [3, 6]. HBV is a DNA virus that gets incorporated into the host genomic DNA. Even though the insertion is random, in some cases HBV infection is enough to induce the development of HCC in the absence of cirrhosis [3, 6]. Still, the most frequent insertion site for HBV is TERT promoter, hence telomerase gets activated upon infection [3]. Moreover, HBV X protein is shown to be able to regulate the important oncogenes such as c-Jun hence being an important effector in progression to HCC [6]. HCV is an RNA virus and its core protein affects the expression of RAS, an important oncogene, and has been shown to dysregulate p53 expression, an important tumor suppressor [6]. Furthermore, chronic infection with HBV and HCV contributes to a non-resolved inflammation in liver which in turn contributes to HCC development.

Multiple signalling pathways are associated with HCC progression. Activating mutation in CTNNB1 gene are frequently found in HCC patients infected with HBV [3, 7]. In these patients there is constitutive active WNT signalling due to active  $\beta$ -catenin. Constitutive active WNT signalling is also observed in patients with inactivating mutations in AXIN1 gene encoding for Axin-1 protein and more rarely in APC, a tumor suppressor gene [7]. RAS/RAF/MAPK and the PI3K–AKT–mTOR pathways are activated in many instances in HCC patients [3, 7]. Inactivating mutations in TSC1/2 (tuberous sclerosis 1/2) and in PTEN (phosphatase and tensin homologue) activate these pathways respectively. On the other hand, mutations in Ras family or BRAF are observed in less than 2% of HCC patients [3]. Other mechanisms altered in HCC include chromatin remodelling with mutations in enzymes epigenetically regulating gene expression and oxidative stress which is frequently found to be constitutively activated [3, 7].

Mutations in tumor suppressor genes are common in HCC patients. Continuous exposure to aflatoxin B1 (AFB) has been linked to p53 mutation and HCC progression [3, 6]. AFB is produced by *aspergillus parasiticus* and *aspergillus flavus*. It can be found in contaminated rice, corn and peanut and when consumed and metabolised is mutagenic [6]. It specifically induces p53 mutation in codon 249, a mutation which is not found in patients not exposed to AFB. Mutation in cyclin-dependent kinase inhibitor 2A (CDKN2A), retinoblastoma 1 (RB1), p16INKa, and hypermethylation in p16 have also been observed in HCC patients contributing to disease progression [3, 6].

### **1.1.2. Surveillance, diagnosis, staging system and therapeutic options for HCC**

HCC development is asymptomatic till disease has progressed to advanced stages. For patients diagnosed at advanced stages, therapeutic options are limited and average overall survival (OS) is 6 months [4]. Hence, for patients at high risk of developing HCC regular surveillance is recommended. Under the high-risk group fall patients with or without cirrhosis but with chronic HBV or HCV infection [5]. Regular surveillance increases the chances of detecting HCC in earlier stages. Hence, patients can receive treatment and OS can be higher. Patients not under surveillance that are diagnosed with HCC have lower OS when compared to the under-surveillance peers due to diagnosis at an advanced stage and lack of therapeutic options [4].

Surveillance of patients for HCC development is performed mainly through abdominal ultrasound [4]. Lately, biomarkers are being used but their efficiency and accuracy remain controversial [4]. Detection of nodes bigger than 1cm in diameter is a sign of possible HCC development in the patient hence proper diagnosis should follow [4]. A diagnosis can be performed by non-invasive approaches such as radiology using MRI or CT or by invasive approaches such as biopsy and staining for HCC specific markers [4].

There are multiple HCC staging systems used in the world such as the Cancer of the Liver Italian Program (CLIP), the Hong Kong classification, the Japan Integrated Staging (JIS), the TNM system and the Barcelona Clinic Liver Cancer (BCLC) system [3, 4, 5]. None of them has been globally accepted but the most used one due to extensive validation is the BCLC system. A summarized representation of the BCLC system is represented in Figure 1.3. Patients with up to 3 nodules of 3cm in diameter

are considered very early or early stage (BCLC 0 and A) [3, 4, 5]. These patients can receive treatment options such as resection, transplantation and ablation [3, 4, 5]. Patients with multiple large tumors but asymptomatic and preserved liver functions are considered intermediate stage (BCLC B). These patients can receive transarterial chemoembolization. For advanced-stage HCC patients (BCLC C) having tumors spread beyond liver and showing cancer-related symptoms, systemic treatment with Sorafenib or Regorafenib are the only treatment options shown to improve survival [3, 4, 5].

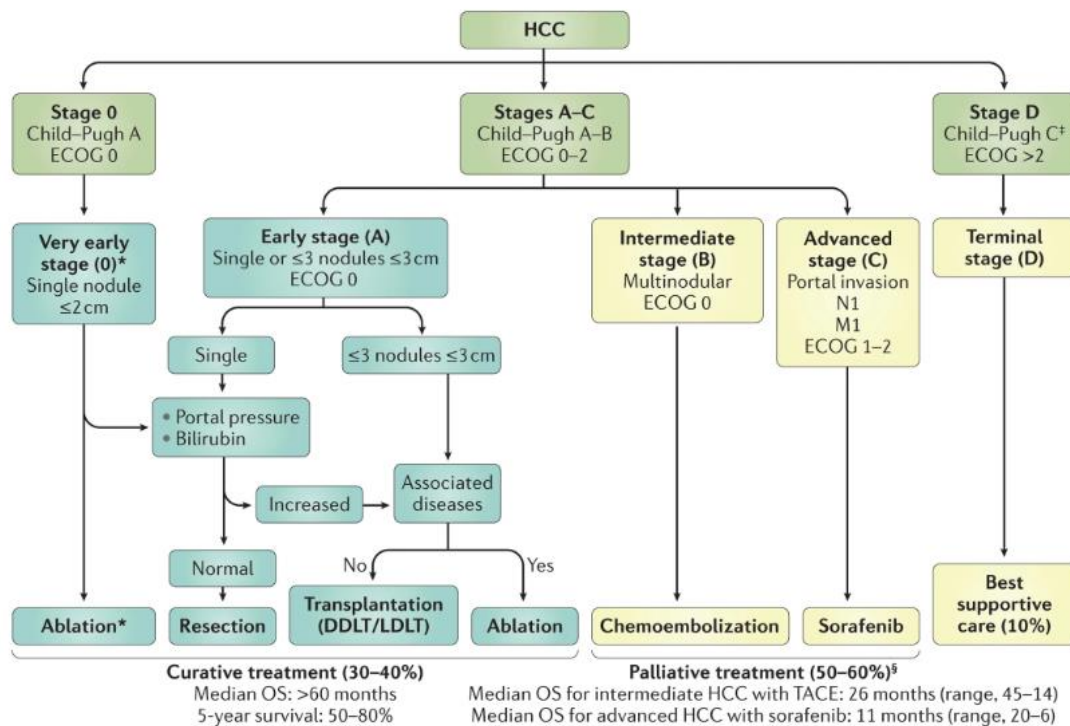


**Figure 1.3:** BCLC staging system for HCC patients. Reproduced with permission from Springer Nature [3].

### 1.1.3. Systemic therapy for advanced HCC patients

Advanced HCC has very poor prognosis due to lack of therapeutic options for patients. Sorafenib (Nexavar) is the only FDA approved systemic therapy for advanced HCC patients. Its approval in 2007 was based on two randomized placebo-controlled phase III trials improving median patient survival from 7.9 months in placebo groups to 10.7 months in treatment groups [7, 9]. Despite the fact that these two trials were in geographically different locations (Sorafenib HCC Assessment Randomized Protocol (SHARP) in Europe, America and Australia and the sorafenib Asia-Pacific (AP) trial

in China, Taiwan and South Korea), they followed same criteria for patient inclusion and exclusion and the overall outcomes were comparable [9, 10]. Since then, Sorafenib is the standard treatment for HCC patients

Sorafenib is an orally administered tyrosine kinase inhibitor [8]. It has been shown to inhibit proliferation of cancer cells, induces cell death and blocks angiogenesis through inhibition of multiple receptor tyrosine kinases such as vascular endothelial growth factor receptor (VEGFR) 1, 2, 3, platelet-derived growth factor receptor  $\beta$  (PDGFR- $\beta$ ), KIT, RET, FLT-3, and some of the serine/threonine kinases in the MAPK signalling pathway including Ras, Raf, pSTAT3 [10, 13]. Moreover, Sorafenib is shown to induce downregulation of Bcl-2 proteins and induce p53 -upregulated-modulator-of-apoptosis hence promoting tumor cell death [10]. Additional data also suggest the role of Sorafenib in modulating an immune response against tumor cells through enhancing tumor-specific T cells [10].

Nonetheless, majority of the advanced HCC patients treated with Sorafenib, eventually develop resistance. In 2017, Regorafenib was approved as a second-line treatment for advanced HCC patients progressing on sorafenib [8]. In phase III trials, regorafenib showed survival benefit and an increase in median survival of patients tolerating sorafenib from 7.8 months in placebo group to 10.6 months [8]. Moreover, in 2019 ramucirumab and in 2020 combinatory treatment with nivolumab and ipilimumab were FDA approved for HCC patients progressing on Sorafenib [79, 80].

#### **1.1.4. Mechanisms of sorafenib resistance**

Despite the fact that Sorafenib is the only approved first-line systemic treatment for HCC patients, it can provide a survival advantage of only 3 months [12, 13]. Development of sorafenib resistance is a limiting factor for patients to fully benefit from treatment with this drug.

There are two types of resistance to Sorafenib: primary resistance and acquired resistance [11]. Primary resistance is due to the genetic heterogeneity of HCC making tumor cells resistant to Sorafenib. Even though the exact mechanisms are unknown, overexpression of EGFR, overactivation of Ras/Raf/MEK/ERK signalling pathway and amplification of VEGFR are some of the main genetic changes contributing to primary resistance to Sorafenib [11]. Furthermore, these molecular changes can be used as biomarkers to predict responsiveness of the patient to the drug.

Acquired resistance develops during treatment with Sorafenib [11]. Tumor cells undergo changes and activate certain mechanisms to overcome Sorafenib-induced cell death. One of the main signalling pathways activated in Sorafenib resistant tumor cells is PI3K/AKT pathway [11, 12]. PI3K/AKT signalling pathway activation provides proliferation and survival properties. Phosphorylation levels of AKT are higher in Sorafenib resistant cells, hence pharmaceutically inhibiting AKT is shown to resensitize cells to Sorafenib. c-Jun is also shown to be activated in Sorafenib resistant cells and similarly its inhibition improves Sorafenib-induced cell death [12].

Microenvironment is shown to be important in development of Sorafenib resistance. A hypoxic environment, common to many solid tumors, selects for transformed cancer cells able to survive under hypoxic conditions. Frequently these cells become extremely resistant to drug therapies including Sorafenib. This resistance is closely related to upregulation of HIF-1 $\alpha$  and HIF-2 $\alpha$  [11, 12].

Epithelial-mesenchymal transition (EMT) is also linked to Sorafenib resistance [11, 12, 13]. EMT occurs under hypoxic conditions in tumors and also under specific signalling such as TGF $\beta$ 1 [13]. EMT is negatively affecting patient survival and contributes to drug resistance. The loop between Sorafenib resistance and EMT is still not fully understood. Sorafenib treatment inhibits EMT but sorafenib resistant tumor cells show reduced epithelial properties such as low E-cadherin and KRT19 expression levels and increase mesenchymal markers such as upregulated vimentin levels becoming more metastatic and invasive [12, 13].

## **1.2. IKBKE gene**

### **1.2.1. The role of IKBKE in innate immunity response.**

IKBKE, also known as IKK $\epsilon$  and IKK-i, is a non-canonical serine/threonine kinase belonging to the inhibitor of  $\kappa$ B (I $\kappa$ B) kinase family (IKK family). Other members of the IKK family include the canonical IKKs, IKK $\alpha$  and IKK $\beta$  which form a complex with NEMO, an adaptor protein also known as IKK $\gamma$ , to activate NF- $\kappa$ B signalling through phosphorylation of I $\kappa$ B and subsequent Lys48-linked polyubiquitination and proteasomal degradation [14, 16]. TBK1 (Tank-binding kinase 1), as IKBKE, is also a non-canonical kinase of IKK family whose first discovery was based on sequence similarities to the canonical kinases and its interaction to TRAF family member-associated NF- $\kappa$ B activator (TANK) [15].

IKBKE gene is located at 1q32 and contains 22 exons and its promoter contains active binding site for both NF- $\kappa$ B and STAT3 [14, 17]. IKBKE is an 80KD protein firstly isolated in 1999 as a novel kinase induced by lipopolysaccharide (LPS) and PMA in mouse macrophages, whereas its amino acid sequence was later analysed by Peters et al [18, 19]. IKBKE has 33% and 31% sequence homology to IKK $\alpha$  and IKK $\beta$  respectively, but 65% homology with TBK1 [14, 15]. Both IKBKE and TBK1 contain similar helix-loop-helix (HLH) and a leucine zipper (LZ) domain important in homo/heterodimerization and a ubiquitin-like domain essential in their kinase activities and regulation of downstream signalling [20]. IKBKE and TBK1 lack the NEMO-binding domain, present in IKK $\alpha$  and IKK $\beta$ , hence they cannot bind to NEMO and become part of the complex that activates NF- $\kappa$ B. Nevertheless, IKBKE and TBK1 are shown to form complexes with other scaffold proteins including TANK, NAK associated protein 1 (NAP1) and similar to NAP and TBK1 adaptor (SINTBAD) [16]. Moreover, it is suggested that IKBKE and TBK1 associate with different scaffold proteins in order to provide signal specificity [16]. An example of such case has been shown in specific interaction of IKBKE and TANK to phosphorylate and activate Interferon regulating factors (IRF) 3 upon LPS stimulation in TLR4 expressing cells [16].

Previous studies have shown that IKBKE is a viral-activated kinase very crucial in innate immune response [21]. It is activated by pattern-recognition receptors (PRR) found in the plasma membrane or cytoplasm of cells such as Toll-like receptors (TLR) 3 and 4 recognizing double stranded viral RNA and LPS respectively and RIG-1 recognizing cytosolic viral RNA [16]. Additionally, IKBKE is shown to be activated upon cytokines such as IL-6, IL-1, IFN- $\gamma$  and TNF [14]. Upon adequate stimuli, IKBKE phosphorylates I $\kappa$ B $\alpha$  in Serine 536 and increase I $\kappa$ B $\alpha$  turnover when overexpressed in cells hence activate the NF- $\kappa$ B pathway [18]. Contradicting these results, IKBKE deficient mouse embryonic fibroblasts (MEFs) showed expected I $\kappa$ B $\alpha$  degradation upon TNF- $\alpha$ , LPS and IL-1 $\beta$  stimulation but deficient upregulation of numerous NF- $\kappa$ B-target genes including IL6, COX2 and MCP1 [22]. Possible reasons behind these results might rely on the fact that IKBKE was also found to phosphorylate p65/RelA subunit of NF- $\kappa$ B in Serine 536 required for further NF- $\kappa$ B activation and transcriptional response [14]. In IKBKE absence, adequate activation of NF- $\kappa$ B is not achieved. Moreover, IKBKE phosphorylates p65 in Serine 468 which further enhances

its activity [14]. Clearly, IKBKE plays a major role in modulating inflammatory responses through NF- $\kappa$ B pathway. However, this regulation of NF- $\kappa$ B cascade is not always positively affected. Studies show that IKBKE and TBK1 are able to phosphorylate the canonical IKKs, IKK $\alpha$  and IKK $\beta$ , in their activation loops and negatively affect their kinase activity. TANK was shown to be necessary in mediating the interaction between these non-canonical and canonical IKKs [23].

In addition to regulating NF- $\kappa$ B signalling, IKBKE phosphorylates IRF3 and 7 in their C-terminal region and more specifically on Ser386, Ser396 and Ser402 of IRF3. IRF-3 and IRF-7 form homo- or heterodimers upon phosphorylation and are translocated to the nucleus where they transcriptionally regulate their target genes mainly type I IFN (IFN- $\alpha$  and IFN- $\beta$ ) [14].

There exists redundancy between IKBKE and TBK1 in IRF3 phosphorylation and activation. However, studies also show differences in their regulation mechanisms such as preferential abolishment of IKBKE activity by MyD88 upon TLR3 signalling [16]. Moreover, TBK1 is constitutively expressed in most tissues while IKBKE is an inducible kinase expressed in specific tissue types. Embryonic knockout of TBK1 in mice is lethal while IKBKE deficient mice are viable supporting the hypothesis that IKBKE and TBK1 control different aspects of signalling [21].

### **1.2.2. The role of IKBKE in oncogenesis**

IKBKE's role in activation of innate immunity has been established by multiple studies proving its importance. However, in recent years, new research has shown that IKBKE is not only involved in the innate immunity response and inflammation but also in oncogenic transformation and has been shown to be upregulated in many cancers including breast cancer, ovarian cancer and colon cancer and to modulate PI3K/AKT pathway, Hippo pathway and WNT signalling in addition to NF- $\kappa$ B pathways.

#### **1.2.2.1. IKBKE expression levels in different cancers**

IKBKE is normally expressed in thyroid, spleen pancreatic tissue, and peripheral blood leukocytes [20]. However, its expression has been related to many cancer types. Different studies on whole genome analysis have shown that IKBKE is highly expressed in both transcriptional and translational levels in multiple breast cancer cell

lines and in primary tumors [24, 25]. Moreover, IKBKE knockdown by using siRNA or its pharmacological inhibitors led to reduction in proliferation of breast cancer cells and cell cycle arrest in G0/G1 phase [26]. ICH staining and comparison of normal and esophageal squamous cancer tissue revealed IKBKE to be upregulated in 84% of cancer tissue [29]. High expression levels of IKBKE were also detected in gliomas through immunohistochemistry (ICH) on primary cancer tissues and IKBKE overexpression was shown to be directly correlating to the stage of glioma development [27]. IKBKE knockdown showed reduction in proliferation and G0/G1 cell arrest and inhibition of migration and invasion in *in vitro* and *in vivo* settings [28]. IKBKE was found to be overexpressed in gastric cancer and pancreatic ductal adenocarcinoma (PDAC) patients as shown by ICH analysis [30, 31, 32]. IKBKE silencing in PDAC cell lines showed inhibition of proliferation *in vitro* and slowed down tumor initiation and progression *in vivo* [33]. Additionally, IKBKE was shown to promote the establishment of an inflammatory tumor microenvironment and stimulated proliferation and cell survival of intestinal cell in colorectal cancer (CRC) [34]. IKBKE knockdown was shown to inhibit proliferation ability of some colorectal cancer cell lines and its overexpression contributed to Vincristine (VCR) resistance on colorectal cancer cells [35]. IKBKE was found to be overexpressed in ovarian cancer cells lines and primary tumor at both the protein and mRNA levels and its silencing resulted in a decrease in proliferation and invasion ability of ovarian cancer cell lines both *in vitro* and *in vivo* [36, 37]. Moreover, IKBKE expression levels were shown to be higher in metastatic carcinomas when compared to primary ovarian carcinomas [37]. Similar results were observed in renal clear cell carcinoma patients were metastatic tissues showed significantly higher IKBKE levels of expression than the primary carcinomas [38]. IKBKE expression levels were analysed by ICH in non-small cell lung cancer (NSCL) tumor samples and results showed IKBKE to be elevated in tumor tissues [39]. Additionally, NSCL cell lines showed elevated IKBKE expression [40]. Moreover, IKBKE expression was associated with smoking statues of the squamous cell carcinoma of lung (SCCL) patients and stage of tumor development in a study were paraffin-embedded tumor samples were analyzed [41]. Other cancer types were IKBKE was shown to be highly elevated include prostate cancer and adenocarcinomas, human T-cell leukemia virus type I (HTLV-1), acute myeloid leukemia (AML), melanoma and endometrial cancer [17]. Moreover, to our knowledge only one research has shown a correlation between IKBKE expression and

hepatocellular carcinoma (HCC). This study performed ICH analysis on primary tumor tissues and concluded that IKBKE was highly expressed (200 out of 220) in tumor tissue when compared to the adjacent non-tumorigenic tissues [42].

### **1.3. IKBKE's association with different pathways in cancer**

#### **1.3.1. IKBKE and NF- $\kappa$ B**

NF- $\kappa$ B is a regulator of hallmarks of cancer through transcriptional regulation of genes contributing to tumor initiation, development, metastasis and drug resistance [43]. NF- $\kappa$ B is constitutively expressed in many different types of human cancers. Constitutively active NF- $\kappa$ B is a consequence on mutations in genes encoding for NF- $\kappa$ B transcription factors or in genes directly controlling NF- $\kappa$ B activation [43]. Moreover, tumor cells secrete cytokines (IL-1 $\beta$ , TNF- $\alpha$ ) that further more activate NF- $\kappa$ B activity to maintain a continuous inflammatory tumor microenvironment [43, 44]. Other stimuli apart from inflammatory cytokines that activate NF- $\kappa$ B include epidermal growth factor (EGF), LPS, viral infection, reactive oxygen species, DNA damage or other oncogenic stress [44]. Upon activation, NF- $\kappa$ B promotes cell proliferation through encoding of G1 cyclins like cyclin D1 and inhibition of apoptosis induced by TNF- $\alpha$  through activation of anti-apoptotic factors such as members of the BCL2 family and FLICE inhibitory protein (c-FLIP) [43]. Moreover, NF- $\kappa$ B promotes metastasis of tumors by activating transcription factors that stimulate epithelial-mesenchymal transition such as Twists1 and Snail [45]. Important involvement of NF- $\kappa$ B in tumor development include its direct regulation of tumor metabolism such as glucose intake through upregulation of GLUT3 and regulation of SCO2, very important in mitochondrial respiration. Lastly, oncogenic mutations in PI3K, EGFR, RAS and p53 promote NF- $\kappa$ B activation in tumor cells [45].

IKBKE is shown to be an activator of NF- $\kappa$ B pathway and display oncogenic properties in multiple cancer types. Different studies show that IKBKE promotes breast cancer tumorigenesis through activation of NF- $\kappa$ B pathway [24, 25, 26]. More specifically, IKBKE was shown to phosphorylate TRAF2 which promoted TRAF2 Lys63-linked polyubiquitination and recruitment and activation of the canonical IKKs, thereby activating NF- $\kappa$ B signalling and stimulating breast cancer development [46]. Moreover, IKBKE was shown to phosphorylate CYLD in breast cancer cell lines which diminished its suppressive impact on TRAF2 and NEMO, hence promoted NF-

$\kappa$ B activation and tumorigenesis [47]. Additionally, IKBKE stimulated the progression of glioma by promoting the translocation to the nucleus of two NF- $\kappa$ B subunits, p50 and p65 [27].

### **1.3.2. IKBKE and PI3K/AKT**

The PI3K/AKT signalling pathway is constitutively activated in many cancers. It is one of the most important signalling pathways controlling cell survival, cell growth, cell metabolism, differentiation and motility in response to a variety of signals coming from G protein-coupled receptors (GPCR) and growth factor receptor tyrosine kinases (RTK) [48]. Oncogenic mutations including PIK3CA, PIK3R1, PTEN, AKT, TSC1, TSC2, LKB1, MTOR and various others contribute to aberrant activation of PI3K/AKT pathway observed in a wide range of cancers [49]. For this reason, a number of PI3K/AKT signalling pathway inhibitors have been approved for clinical use to chemotherapeutically treat cancer patients [48]. Examples of such drugs in use include temsirolimus, everolimus, idelalisib, and copanlisib [48].

IKBKE has been reported to activate AKT through direct phosphorylation on Ser-473, in AKT's hydrophobic motif, and THR-308, in AKT's activation loop, hence activating downstream signalling and promoting tumorigenesis [50].

A study in PDAC cell lines showed that IKBKE promote c-Myc nuclear translocation through phosphorylation and activation of a cascade involving AKT, GSK3 $\beta$  and lastly c-Myc, hence promoting tumorigenesis and metastatic potential of the cells [33]. Moreover, IKBKE was shown to be able to provide reactivation of AKT in mTOR inhibited PDAC cells contributing to insensitivity to mTOR inhibitors [51]. In breast cancer cell lines, TNF-dependent IKBKE expression was shown to be dependent on AKT2 activity where AKT2 deficient cells were unable to upregulate IKBKE upon TNF stimulation and AKT2 overexpressing cells increased IKBKE expression. Furthermore, IKBKE was downstream of AKT2 signalling, promoting breast cancer cell growth and survival [52]. Another study on breast cancer and NSCLC cells reported that IKBKE was able to phosphorylate FOXO3a, an important transcription factor downstream of AKT with known tumor suppressor roles, on Ser-644. Upon phosphorylation by IKBKE, FOXO3a is degraded hence apoptosis is inhibited and cell proliferation is promoted [53]. Such studies have shown that direct phosphorylation

and activation of AKT by IKBKE and regulation of downstream signalling is a possible mechanism of IKBKE contributing to oncogenesis.

### **1.3.3. IKBKE and HIPPO signalling pathway**

Hippo signalling controls multiple function including tissue growth, tissue regeneration, and cell fate. Perturbation in the Hippo signalling and mutations or altered expression of genes related to Hippo signalling have been shown to promote tumorigenesis. Some of the main kinases involved in the Hippo signalling include mammalian Ste20-like kinases 1/2 (MST1/2), large tumor suppressor 1/2 (LATS1/2), yes association protein (YAP) and TAZ, its paralog [55]. Hippo signalling can be regulated upon a variety of intracellular and extracellular signalling including mechanical stress, cell adhesion, GPCRs such as lysophosphatidic acid (LPA) and sphingosine 1-phosphate (S1P) and EGFR and VEGFR signalling [54, 55]. Upon activation of the Hippo pathway, phosphorylated MST1/2 activates LATS1/2, which then in turn phosphorylates YAP/TAZ inhibiting their activity [42].

Recently, multiple studies have shown a role of IKBKE in regulating Hippo pathway through interactions with the kinases involved in this signalling pathway. IKBKE is shown to interact and phosphorylate YAP protein upon TNF $\alpha$  stimulation in MCF7, a breast cancer cell line. Moreover, IKBKE overexpression promoted YAP interaction to TEAD transcription factors [56]. In glioblastoma cell lines, IKBKE was shown to directly interact to YAP1 and TEAD2 and IKBKE downregulation inhibited EMT transition through Hippo pathway [57]. Additionally, the same research group showed that IKBKE regulated Hippo signalling by promoting the degradation of LATS1/2 kinases and inactivation of Hippo pathway, hence Amlexanox, IKBKE inhibitor, suppressed glioblastoma tumor growth [58]. Moreover, IKBKE was shown to promote the translocation of YAP1 to nucleus by preventing its phosphorylation on Ser127 and degradation, thereby promoting glioblastoma progression [58].

### **1.3.4. IKBKE and other pathways**

IKBKE was demonstrated to be downstream of Epidermal Growth Factor Receptor (EGFR) and interacting with it in NSCLC cells lines [40]. Moreover, it was shown that IKBKE was activated by mutated EGFR through phosphorylation on two residues, Tyr153 and Tyr179, thereby promoting proliferation, invasion and resistance to EGFR inhibitors of NSCLC cells lines in both *in vitro* and *in vivo* settings [40]. In breast

cancer cells, knockdown of IKBKE negatively affected the EGFR expression levels, an association which was also shown through ICH in breast cancer specimens [59]. Moreover, IKBKE deficiency in  $\beta$ -catenin activated models of intestinal cancer development resulted in less tumor incidences and prolonged survival [34]. This study also shows that IKBKE promotes the establishment of an inflammatory microenvironment in intestine, hence promoting tumorigenesis [34].

## CHAPTER 2

### Materials and Methods

#### 2.1. Materials

All materials used in this study are mentioned in the sections below.

##### 2.1.1. Chemical and reagents

A full list of all the chemicals and reagents used throughout this study can be found in Table 2.1.

**Table 2.1.** Chemicals and reagents used in this study.

Product name:	Catalog No:	Company, Country
2-mercaptoethanol	M3148	Sigma-Aldrich, USA
2-Propanol	100995	Merck, Germany
40% Acrylamide/Bis Solution 37.5:1	1610148	Bio-Rad, USA
Ammonium persulphate	A2941	Applichem, USA
Bovine Serum Albumin	sc-2323	Santa Cruz Biotechnology, USA
cOmplete, Protease inhibitor cocktail tablets	11697498001	Roche, USA
Dimethyl sulfoxide	A3672	Applichem, Germany
Ethanol	32221	Sigma-Aldrich, USA
Glycine	GLN001.1	Bioshop, Canada
Glycerol	15524	Sigma-Aldrich, USA
Hydrochloric acid	100317	Merck, Germany
Immobilion-P PVDF Membrane	1620177	Bio-rad, USA
NaOH	106.462	Merck, Germany
PageRuler Prestained Protein Ladder	26616	Thermo Scientific, USA

**Table 2.1.** Chemicals and reagents used in this study.

Product name:	Catalog No:	Company, Country
polyFect	1015586	Qiagen, Germany
Poly(2-hydroxyethyl methacrylate) (polyHEMA)	P3932-10G	Sigma-Aldrich, USA
Propidium iodide (PI)	P4170	Sigma-Aldrich, USA
Ribonuclease A	R6513	Sigma-Aldrich, USA
SDS	71725	Sigma-Aldrich, USA
Sodium Azide	S2002-5G	Sigma-Aldrich, USA
TEMED	1610801	Bio-rad, USA
Tris (Trizma Base)	T1503	Sigma-Aldrich, USA
Triton X-100	T8787	Sigma-Aldrich, USA
Tween-20	822184	Merck, Germany
XenoLight D-Luciferin Firefly, Potassium Salt	122799	PerkinElmer, USA
Cell Proliferation Reagent WST-1	05015944001	Roche, USA

### 2.1.2. Kits

A list of all the kits used throughout this study can be found in Table 2.2.

**Table 2.2.** Kits used in this study.

Product name:	Catalog No:	Company, Country
CellTiter-Glo® Luminescent Cell Viability Assay	G7571	Promega, USA
CellTiter-Glo® 3D Cell Viability Assay	G9683	Promega, USA
Click-iT Plus EdU Alexa Fluor 488 Flow Cytometry Assay Kit	C10633	Invitrogen, USA
E.Z.N.A. Plasmid DNA Maxi Kit	D6922-02	Omega bio-tek, USA

**Table 2.2.** Kits used in this study.

Product name:	Catalog No:	Company, Country
E.Z.N.A. Plasmid DNA Mini Kit	D6943-01	Omega bio-tek, USA
E.Z.N.A. Total RNA Kit I	R6834-02	Omega bio-tek, USA
eBioscience Annexin V-FITC Apoptosis Detection Kit	BMS500FI/300	Invitrogen, USA
iScript cDNA Synthesis Kit	170-8891	Bio-Rad, USA
LightCycler® SYBR® Green Master	480 04887352001	Roche Diagnostics, USA
LookOut Mycoplasma PCR detection kit	MP0035	Sigma-Aldrich, USA
Pierce BCA Protein Assay Kit	23227	Thermo Scientific, USA
Pierce ECL Western Blotting Substrate	32106	Thermo Scientific, USA
SuperSignal West Femto Maximum Sensitivity Substrate	34095	Thermo Scientific, USA
SYBR Premix Ex Taq II (Tli RNaseH Plus), Bulk	RR820L	TaKaRa, Japan

### 2.1.3. Cell culture components

A list of all the components used in culturing cells can be found in Table 2.3.

**Table 2.3.** Cell culture media, chemicals and reagents used in the study.

Product name:	Catalog No:	Company, Country
Animal-Free Recombinant Human EGF	AF-100-15	Peptrotech, USA

**Table 2.3.** Cell culture media, chemicals and reagents used in the study.

Product name:	Catalog No:	Company, Country
Amlexanox	A2401	Tokyo Chemical Industry, Japan
Corning Matrigel Basement Membrane Matrix Growth Factor Reduced, Phenol Red Free	356231	Corning, USA
Dharmacon Trans-Lentiviral Packaging Kit with Calcium Phosphate Transfection Reagent	TLP5912	GE Healthcare, UK
Dimethyl sulfoxide	A3672	Applichem, Germany
Dulbecco's Phosphate Buffered Saline	BE17-512F	Lonza, Switzerland
DMEM with Glucose and L-Glutamine	12-604F	Lonza, Switzerland
Fetal Bovine Serum Heat Inactivated	S181H-500	Biowest, USA
Hiperfect Transfection Reagent	301705	Qiagen, Germany
HyClone Phosphate Buffered Saline	SH30258.02	GE Healthcare, UK
L-Glutamine	BE17-605E	Lonza, Switzerland
Lipofectamine™ 2000 Transfection Reagent	11668027	Invitrogen, USA
Opti-MEM I	31985-070	Gibco, USA
Pen-Strep	DE17-602E	Lonza, Switzerland
Polybrene	sc-134220	Santa Cruz Biotechnology, USA

**Table 2.3.** Cell culture media, chemicals and reagents used in the study.

Product name:	Catalog No:	Company, Country
PolyFect Transfection Reagent	301105	Qiagen, Germany
Puromycin	ant-pr-1	Invivogen, USA
Recombinant TGF- $\beta$ 1 (HEK293 derived)	100-21	Peptotech, USA
Trypsin-EDTA	BE17-161E	Lonza, Switzerland
Trypsin-EDTA	25200056	Gibco, USA
RPMI 1640	BE12-167F	Lonza, Switzerland)
Sorafenib	S7397-200MG	Selleckchem, USA

#### 2.1.4. Buffers

Buffers used in this study and their composition have been listed on Table 2.4.

**Table 2.4.** Buffers and their compositions.

Buffer:	Composition:
Cell Lysis Buffer (1x)	5mL 2X cell lysis buffer stock (2x), 500 $\mu$ L Na <sub>3</sub> VO <sub>4</sub> , 500 $\mu$ L NaF, 500 $\mu$ L $\beta$ -Glycerophosphate, 500 $\mu$ L cOmplete protease inhibitor up to 10mL water
Cell Lysis Buffer Stock (2x)	25mL 1M HEPES, 30mL 5M NaCl, 5mL Triton-X-100, 100mL Glycerol 340mL water
Crystal Violet solution (0.5%)	0.5gr Crystal Violet, 25mL methanol, 75mL water.
HBSS (2x)	10mL 1M HEPES, 666 $\mu$ L 3M KCl, 0.4g Dextrose, 11.2mL 5M NaCl, 0.0531g Na <sub>2</sub> HPO <sub>4</sub> , up to 200mL water pH=7.01
LB Broth	10gr NaCl; 5gr Yeast Extract; 10gr Tryptone

**Table 2.4.** Buffers and their compositions.

Buffer:	Composition:
LB Agar	10gr NaCl; 5gr Yeast Extract; 10gr Tryptone; 15gr Bacto agar
Mild Stripping Buffer	3g Glycine, 0.2g SDS, 20mL Tween, up to 200mL water, pH= 2.2
PBS (1x)	1.702g Na <sub>2</sub> HPO <sub>4</sub> , 8g NaCl, 0.2g KCl, 0.2g KH <sub>2</sub> PO <sub>4</sub> , up to 1L water
Protein Loading Dye (2x)	6.25ml 1M Tris-HCl pH:6.8; 25ml 10% SDS; 10ml β-Mercaptoethanol; 20ml glycerol; 0.008% Bromophenol blue
Protein Loading Dye (4x)	12.5ml 1M Tris-HCl pH:6.8; 5gr SDS; 5ml β-Mercaptoethanol; 10ml glycerol; 0.004% Bromophenol blue
Running Buffer (10x)	144g Glycine, 10 gr SDS, 30.2g Tris-Base, up to 1L water
Separating Gel (7%)	1.4mL Bis-Acrylamide, 3.1mL water, 0.75mL Glycerol, 1.875mL 1.5M Tris pH=8.8, 187.5μL 0.25M EDTA, 150μL 10% SDS, 62.5μL 10% APS, 7.5μL TEMED
Stacking Gel	0.3mL Bis-Acrylamide, 1.75mL water 312.5μL 1M Tris pH=6.8, 62.5μL 0.25M EDTA, 50μL 10%SDS 30μL 10% APS, 5μL TEMED
TBS-T (10x)	24.2g Tris-Base, 80g NaCl set pH=7.6 20mL Tween, up to 1L water
Transfer Buffer (10x)	144g Glycine, 30.2g Tris-Base, up to 1L water

### 2.1.5. Antibodies

Antibodies used in this study have been listed on Table 2.5.

**Table 2.5.** Antibodies used in this study.

Product name:	Catalog No:	Company, Country
Actin Antibody (C-2)	sc-8432	Santa Cruz Biotechnology, USA
Anti-alpha smooth muscle Actin	ab5694	Abcam, UK
Anti-mouse IgG, HRP- linked Antibody	7076	Cell Signaling Technology, USA
Anti-rabbit IgG, HRP- linked Antibody	7074	Cell Signaling Technology, USA
Akt Antibody	9272	Cell Signaling Technology, USA
c-Myc (D84C12) Rabbit mAb	5605	Cell Signaling Technology, USA
E-cadherin Antibody (G- 10)	sc-8426	Santa Cruz Biotechnology, USA
ERK 1 Antibody (G-8)	sc-271269	Santa Cruz Biotechnology, USA
GAPDH Antibody (0411)	sc-47724	Santa Cruz Biotechnology, USA
IKK $\epsilon$ (D20G4) Rabbit mAb	2905	Cell Signaling Technology, USA
Integrin $\alpha$ 5 Antibody	4705	Cell Signaling Technology, USA
Monoclonal Anti- $\alpha$ - Tubulin antibody produced in mouse	T5168	Sigma-Aldrich, USA
N-Cadherin (13A9) Mouse mAb	14215	Cell Signaling Technology, USA
PCNA (PC10) Mouse mAb	2586	Cell Signaling Technology, USA
Phospho-Akt (Ser473) (D9E) XP® Rabbit mAb	4060	Cell Signaling Technology, USA

**Table 2.5.** Antibodies used in this study.

Product name:	Catalog No:	Company, Country
Phospho-IKK $\epsilon$ (Ser172) (D1B7) Rabbit mAb	8766	Cell Signaling Technology, USA
Phospho-p44/42 MAPK (Erk1/2) (Thr202/Tyr204) (D13.14.4E) XP $\text{\textcircled{R}}$ Rabbit mAb	4370S	Cell Signaling Technology, USA
Phospho-SAPK/JNK (Thr183/Tyr185) (G9) Mouse mAb	9255S	Cell Signaling Technology, USA
Phospho-TBK1/NAK (Ser172) (D52C2) XP $\text{\textcircled{R}}$ Rabbit mAb	5483	Cell Signaling Technology, USA
TANK Antibody (D-2)	sc-166643	Santa Cruz Biotechnology, USA
TBK1/NAK Antibody	30133	Cell Signaling Technology, USA
Twist Antibody (Twist2C1a)	sc-81417	Santa Cruz Biotechnology, USA
Vimentin (D21H3) XP $\text{\textcircled{R}}$ Rabbit mAb	5741S	Cell Signaling Technology, USA
YAP/TAZ (D24E4) Rabbit mAb	8418	Cell Signaling Technology, USA
ZEB1 Antibody (H-102)	sc-25388	Santa Cruz Biotechnology, USA
ZO-1 (D6L1E) Rabbit mAb	13663S	Cell Signaling Technology, USA

### 2.1.6. Primers

Primers used in this study have been listed on Table 2.6.

**Table 2.6.** Primers used in this study.

Primer:	Sequence:
CDH1 F	CCCGGGACAACGTTTATTAC
CDH1 R	GCTGGCTCAAGTCAAAGTCC
CDH2 F	ACAGTGGCCACCTACAAAGG
CDH2 R	CCGAGATGGGGTTGATAATG
CLAUDIN7 F	CCACTCGAGCCCTAATGGTG
CLAUDIN7 R	GGTACCCAGCCTTGCTCTCA
EPCAM F	CGCAGCTCAGGAAGAATGTG
EPCAM R	TGAAGTACTACTGGCATTGACG
FN F	CTGGCCGAAAATACATTGTAAA
FN R	CCACAGTCGGGTCAGGAG
GAPDH F	GCCCAATACGACCAAATCC
GAPDH R	AGCCACATCGCTCAGACAC
IKBKE 1 F	TGCGTGCAGAAGTATCAAGC
IKBKE 1 R	TACAGGCAGCCACAGAACAG
IKBKE 2 F	CTGCATCCCGACATGTATGA
IKBKE 2 R	CCGGTACATGATCTCCTTGTT
IKBKE 3 F	GAGCATCTACAAGCTGACAGAC
IKBKE 3 R	CAATGCTCCAGAGATCCACAG
KRT18 F	TGATGACACCAATATCACACGA
KRT18 R	GGCTTGTAGGCCTTTTACTTCC
KRT19 F	CTTCCGAACCAAGTTTGAGAC
KRT19 R	GAATCCACCTCCCACTGAC
MMP9 F	GAACCAATCTCACCGACAGG
MMP9 R	GCCACCCGAGTGTAACCATA
SNAI2 F	TGGTTGCTTCAAGGACACAT
SNAI2 R	GTTGCAGTGAGGGCAAGAA
TANK 1 F	CAAAGCCCTCAAATCTCGTAAAC
TANK 1 R	GTCCAGAAGTGGGAAGCTATTT
TANK 2 F	CAGCTGTCACTTCAACAGACTA
TANK 2 R	GCAGAGGAACACAGCCATAA
TBK1 1 F	GTGGTGGGTGGAATGAATCAT

**Table 2.6.** Primers used in this study.

Primer:	Sequence:
TBK1 1 R	ATCACGGTGC ACTATAACCATTCTC
TBK1 2 F	CAACCTGGAAGCGGCAGAGTTA
TBK1 2 R	ACCTGGAGATAATCTGCTGTCTCGA
TBK1 3 F	GAAGGGCCTCGTAGGAATAAAG
TBK1 3 R	CCCGAGAAAGACTGCAAGAA
VIMENTIN F	GGTGGACCAGCTAACCAACGA
VIMENTIN R	TCAAGGTCAAGACGTGCCAGA
ZEB1 F	GGGAGGAGCAGTGAAAGAGA
ZEB1 R	TTTCTTGCCCTTCCTTTCTG
ZEB2 F	AAGCCAGGGACAGATCAGC
ZEB2 R	CCACACTCTGTGCATTTGAACT
ZO-1 F	CAGAGCCTTCTGATCATTCCA
ZO-1 R	CATCTCTACTCCGGAGACTGC

## 2.2. Methods

### 2.2.1. Cell lines, cell culture and reagents

Cell line used in this study is HepG2, kindly received from Prof. Florian Greten. Mycoplasma testing is conducted to ensure cells are not contaminated and analysis on their morphology and proliferation were performed before conducting experiments.

### 2.2.2. Cryopreservation

Cells intended to be stored or stocked for long time periods are cryopreserved. 10% DMSO is used as cryoprotectant agent in the freezing medium (100% FBS). Once cells are carefully collected and centrifuged (1000rpm, 5 minutes at RT), supernatant is removed and the pellet of the cells is resuspended in the freezing medium with a maximum cell density of 1million cells/mL. 1-2mL of cell suspension is added on the cryovials. Cryovials of cells are placed into the Mr. Frosty Cell Freezing Container and placed directly at -80°C. Cells are kept at -80°C for short-term storage and at N<sub>2</sub> liquid for long-term storage.

### 2.2.3. Recovery of cryopreserved cells

The frozen cryovials are warmed rapidly in a water bath set at 37°C. Just before they completely thaw, the cryovials are sterilized, opened and full growth medium is slowly added to completely thaw the cells. Depending on the cell status and fragility, centrifugation (1000rpm, 5 minutes at RT), is or is not performed in order to wash the cells of the DMSO. Lastly the cells are plated into appropriate dish in their full growth medium.

#### **2.2.4. Cell maintenance and propagation**

HepG2 cells are maintained in RPMI growth medium (Lonza) supplemented with 10% Fetal Bovine Serum (FBS) and 1% Penicillin/Streptomycin. Growth medium is changed regularly every 2-3 days and cells are passaged when they reach 80-90% confluency with a subcultivation ratio of maximum 1/4. Cells are incubated at 37 °C, 5% CO<sub>2</sub> and humid cell incubators.

#### **2.2.5. Lentiviral shRNA/CRISPR-Cas9 transfection/ transduction**

HEK293T are used as lentiviral producer cell line. They are cultured in DMEM High Glucose (Lonza) supplemented with 8% FBS. At 70% confluency in a 6cm dish, calcium chloride transfection is used to transfect them with plasmids containing the shRNA/CRISPR-cas9 targeting the gene of interest (Table 2.8.) and packaging plasmids that generate the lentiviral particles. The amounts of the components for calcium phosphate transfection can be found on Table 2.7. The DNA and CaCl<sub>2</sub> are prepared as a separate mixture. 2xHBSS is then added dropwise while the CaCl<sub>2</sub>-DNA mixture is being vortexed at room temperature. After a 15-minute incubation period the mixture is added on top of HEK293T cells. 16 hours post transfection the medium of HEK293T cells is changed. 72 hours post transfection the HEK293T medium containing the viral particles is collected, filtered through 0.2µm filters (Sartorius AG) and added on top of the recipient cells, HepG2, seeded one day prior to reach 30% confluency. Polybrene at a concentration of 10µg/mL is used to improve transduction efficiency. The medium containing lentiviral particles is left on HepG2 cells for two days then removed. To select the efficiently transduced HepG2 cells, 7µg/mL Puromycin is used throughout all the time the cells are kept in culture. CRISPR/Cas9 HepG2 cells are polyclonal. Single colony selection is not performed before experimentation.

**Table 2.7.** Components for calcium phosphate transfection and their amounts.

Component:	Amount:
shRNA / CRISPR/cas9 plasmids	9 $\mu$ g
Packaging plasmid 1: VSVG	3 $\mu$ g
Packaging plasmid 2: R891	6 $\mu$ g
CaCl <sub>2</sub> (2M)	38 $\mu$ L
HBSS (2x)	300 $\mu$ L
ddH <sub>2</sub> O	Up to 600 $\mu$ L

**Table 2.8.** List of plasmids used in lentiviral transfection.

shRNA plasmids*:	CRISPR/cas9 plasmids*:
shRNA scramble = scr_IKK $\epsilon$	CRISPR scramble = CRscr_IKK $\epsilon$
shRNA-29 IKK $\epsilon$ = 29_IKK $\epsilon$	CRISPR-35 IKK $\epsilon$ = CR35_IKK $\epsilon$
shRNA-43 IKK $\epsilon$ = 43_IKK $\epsilon$	CRISPR-12 IKK $\epsilon$ = CR12_IKK $\epsilon$
shRNA-67 IKK $\epsilon$ = 67_IKK $\epsilon$	CRISPR-1314 IKK $\epsilon$ = CR1314_IKK $\epsilon$
	CRISPR-1.1 IKK $\epsilon$ = CR1.1_IKK $\epsilon$
	CRISPR-2.2 IKK $\epsilon$ = CR2.2_IKK $\epsilon$

\*Numbering on the plasmids is random.

### 2.2.6. IKK $\epsilon$ overexpression

HepG2 cells are seeded to reach 60% confluency in 3cm dishes the following day. 2 $\mu$ g of empty plasmid (pcDNA), IKK $\epsilon$ -Myc overexpressing plasmid or IKK $\epsilon$ (KD)-Myc overexpressing plasmid are transiently transfected using Lipofectamine transfection reagent according to the manufacturer protocol. 24h post transfection, the transfected cells are seeded for further analysis or RNA and protein samples are taken.

### 2.2.7. CellTiter-Glo Luminescent cell viability assay

For end-point cell viability analysis, CellTiter-Glo Luminescent cell viability assay (Promega) was used. The CellTiter-Glo Luminescent cell viability assay quantifies the viable, metabolic cells through detection of ATP present in them. Cells are seeded in 96-well plate formats. Cells are treated and viability upon treatment is assessed following the protocol provided by the kit. The luminescence reading is performed in opaque-walled 96-well plates using Synergy HT Microplate reader.

### **2.2.8. Cell Proliferation Reagent WST-1**

For cell proliferation analysis of cells seeded in polyHEMA coated plates, Cell Proliferation Reagent WST-1 (Roche) was used. The Cell Proliferation Reagent WST-1 is based on the activity of cellular mitochondrial dehydrogenase to cleave tetrazolium salt to formazan dye which is directly proportional to the number of alive cells. Cells are seeded in 96-well plate formats and the manufacture's protocol is followed. Formazan dye can be detected by measuring absorbance at 440nm using Synergy HT Microplate reader.

### **2.2.9. Real Time Cell Analysis (RTCA) - Proliferation**

RTCA is a novel technique used to analyse cell proliferation in real time using xCELLigence® Real-Time Cell Analyzer instrument (ACEA Biosciences, San Diego, CA, USA). HepG2 cells are seeded at a density of 8000 cells/well into the wells of E-plate according to manufacturer's protocol and cell proliferation was monitored for 48 hours. Data are normalized to the first possible time point to assure cell seeding differences do not affect the final proliferation results.

### **2.2.10. Colony Formation Assay**

HepG2 cells were seeded at a density of 2000 cells/well in 12-well plate format. Cells medium was changed regularly and colony formation was observed. When colonies reached a density of more than 50 cells/colony, cells were fixed with 100% methanol for 10 minutes at -20°C and stained with 0.5% Crystal violet for 20 minutes at RT. The wells were scanned or pictures were taken and colonies were counted using Colony counter (settings: threshold: 100, minimum: 20, Gray width:50).

### **2.2.11. Anchorage independent growth assay**

2 weeks prior to cell seeding, 96-well plates are double coated with 35uL of polyHEMA (10mg/mL in 95% EtOH) and the plates were incubated in a non-humid incubator at 37 °C till ethanol fully evaporated and coating is formed. Final amount of polyHEMA on the surface of the dish is 0.7mg. HepG2 cells are seeded at a cell density of 3000 cells/well. Daily images of the wells were taken using inverted microscope and cell proliferation was measures using WST-1 assay.

### **2.2.12. Cell cycle analysis through Propidium Iodide staining.**

HepG2 cells are seeded in 3cm dish to reach 70% confluency next day. 24h after seeding, cells are trypsinized, collected and kept on ice at all time. Following washing with cold 1xPBS, cells are fixed using ice-cold 70% freshly prepared ethanol. Ethanol is added dropwise on top of the pellet of cells while vortexing then cells are incubated in ice for 20 minutes. Ethanol is washed away using 1xPBS. Cells are pelleted and washed twice with 1xPBS. To ensure specific binding of the PI only to DNA, cells are incubated for 15 minutes at 37°C with 50µL of 100µg/mL Ribonuclease A(Sigma-Aldrich). 200µL of 50µg/mL PI (Sigma-Aldrich) is added on top (final volume=250 µL). BD Accuri™ C6 Cytometer and NovoExpress cell cycle analysis module are used to analyse the cells for cell cycle distribution.

### **2.2.13. Wound healing assay**

HepG2 cells are seeded in 12 or 24 well plate formats to reach 100% confluency next day. 24 hours after seeding and at 100% confluency wound was introduced using 200uL tip. Wound healing is observed for 72h and images are taken to document it. The gap area was measured using ImageJ MRI Wound\_Healing\_Tool.

### **2.2.14. Western Blotting**

Total protein is isolated using cell lysis buffer. Protein concentration is determined using BCA Protein Assay Reagent Kit (Thermo Scientific, Rockford, IL) according to the manufacturer's instructions. Absorbance readings are performed using Synergy HT microplate reader at 562nm. Protein lysate is mixed with 2x or 4x loading dye and denatured at 75°C for 10 minutes. SDS-PAGE is used to separate the protein samples. Equal amounts of protein are loaded from each sample into each lane of SDS-PAGE. Proteins are transferred to PVDF-membranes through wet transfer. Blocking of the membranes is performed at RT for 30minutes using 10% milk solution in TBS-T 1x. Washing of the membranes is done using TBS-T 1x. Following blocking and washing, membranes are incubated in primary antibodies then secondary antibodies linked to HRP enzyme. Pierce ECL western blotting substrate (Thermo Fisher Scientific, USA) is used to develop the membranes in Amersham™ Imager 600 (Cytiva, UK).

### 2.2.15. Real-Time PCR

Total RNA was isolated using E.Z.N.A. Total RNA Kit I (Omega Bio-Tek, USA) according to manufacturer's instructions. The concentration of RNA was measured using NanoDrop™ One/OneC Microvolume UV-Vis Spectrophotometer (ThermoFisher Scientific). iScript cDNA Synthesis Kit (Bio-Rad, USA) is used to synthesise 1µg of RNA into cDNA following manufacturer's instructions in Techne thermal cycler. Synthesized cDNA is diluted 1:4 in ddH<sub>2</sub>O. RT-PCR mixture is prepared as explained in the Table 2.9. and run in Light Cycler® 480 II (Roche). The reaction conditions are set as explained in TaKaRa or Roche SYBR Green manuals.

**Table 2.9.** Components in RT-PCR mixture.

Component:	Volume:
cDNA	1µL
ddH <sub>2</sub> O	3µL
SYBR Green (TaKaRa/Roche)	5µL
Primer mixture (Forward/Reverse primers=10µM)	1µL

## CHAPTER 3

### Results

#### **3.1. HepG2 cell proliferation negatively correlates to IKK $\epsilon$ expression.**

Our group previously reported that proliferation of Hep3B cells, another HCC cell line, increases upon IKK $\epsilon$  depletion [71]. In the same way, our studies with IKK $\epsilon$ -depleted HepG2 cells has yielded similar results. In Figure 3.1 A and B, viability of IKK $\epsilon$ -depleted HepG2 cells was analysed. IKK $\epsilon$ -depleted HepG2 cells via lentiviral shRNA (Figure 3.1 A) or CRISPR/Cas9 IKK $\epsilon$  (Figure 3.1 B) were both observed to proliferate more when compared to corresponding control cells as measured by Cell-Titer Glo luminescent cell viability -assay. Moreover, proliferative ability of lentiviral shRNA IKK $\epsilon$ -depleted HepG2 cells was analysed using RTCA where IKK $\epsilon$ -depleted cells proliferate significantly more than control cells (Figure 3.1 C). Additionally, colony formation ability increases in shRNA IKK $\epsilon$ -depleted HepG2 cells (Figure 3.1 D) and cell population in S-phase, is increased in CRISPR/Cas9 IKK $\epsilon$ -depleted HepG2 cells (Figure 3.1 E). The opposite is observed in IKK $\epsilon$  overexpressing HepG2 cells where the population of the cells in S phase decrease by 5% (Figure 3.1 F) Despite the increase in proliferation, phosphor-AKT levels decrease in IKK $\epsilon$ -depleted cells and are upregulated upon IKK $\epsilon$  overexpression in HepG2 cells (Figure 3.1 G).

#### **3.2. HepG2 cells show more anchorage independence growth upon IKK $\epsilon$ depletion.**

To assess the effect of IKK $\epsilon$  on anchorage independent growth, control or IKK $\epsilon$  -depleted HepG2 cells were seeded on the polyHEMA coated 96 well plates. Images are taken at day 3, 5 and 7 post-seeding and show a difference in the growth pattern of IKK $\epsilon$  depleted cells compared to control cells (Figure 3.2. A). To quantify anchorage independent growth, stainings at day 1, 3, 5 and 7 was performed with WST-1 reagent. (Figure 3.2 B and C). Anchorage independent growth of HepG2 cells improves upon IKK $\epsilon$  depletion. In shRNA IKK $\epsilon$  depleted HepG2 cells we can also see a trend but it

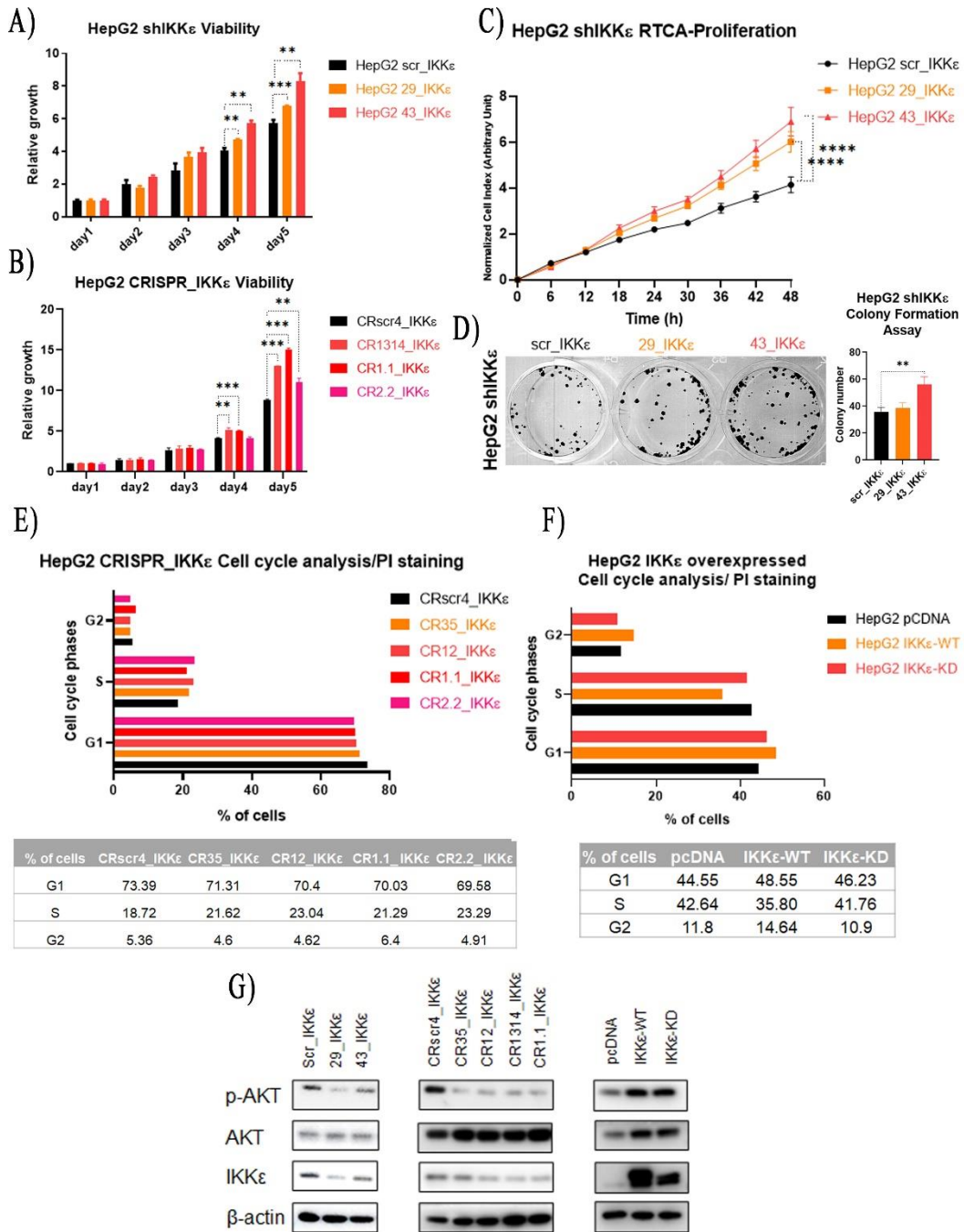


**Figure 3.1: HepG2 cell proliferation negatively correlates to IKK $\epsilon$  expression.** Cell viability in HepG2 cells, in which IKK $\epsilon$  is depleted via **A)** shRNA or **B)** CRISPR/Cas9, is measured using Cell-Titer Glo Luminescent cell viability assay for 5 consecutive days. Data shown are mean  $\pm$  SD of triplicate wells representative of two independent experiments; multiple t-test using Holm-Sidak method; ns not significant, \*  $p < 0.05$ , \*\*  $p < 0.01$ , \*\*\*  $p < 0.001$ , \*\*\*\*  $p < 0.0001$ . **C)** Cell growth in control or shRNA IKK $\epsilon$ -depleted HepG2 cells were analysed via Real Time Cell Analysis (RTCA). Data shown are mean  $\pm$  SD of duplicate wells representative of one experiment; linear regression, differences in slope ns not significant, \*  $p < 0.05$ , \*\*  $p < 0.01$ , \*\*\*  $p < 0.001$ , \*\*\*\*

p<0.0001 **D)** Colony formation assay on shRNA IKK $\epsilon$ -depleted HepG2 cells. Quantification on the right. **E-F)** Cell cycle distribution of control and CRISPR/Cas9 IKK $\epsilon$ -depleted HepG2 cells or IKK $\epsilon$  overexpressing HepG2 cells is analysed through PI staining. Data are representative of one experiment of 100.000 Cells/condition. **G)** Western blot image showing AKT phosphorylation level in shRNA, CRISPR/Cas9 IKK $\epsilon$ -depleted HepG2 cells and IKK $\epsilon$ -overexpressing HepG2 cells.

is not significant (Figure 3.2. B) but in CRISPR/Cas9 IKK $\epsilon$  depleted HepG2 cells this increase in anchorage independent growth is significant. Additionally, integrin  $\alpha$ V, a very important integrin regulating anchorage-independent potential of the cells [60], appears to be downregulated upon CRISPR/Cas9 IKK $\epsilon$  depletion in HepG2 cells (Figure 3.2 D).

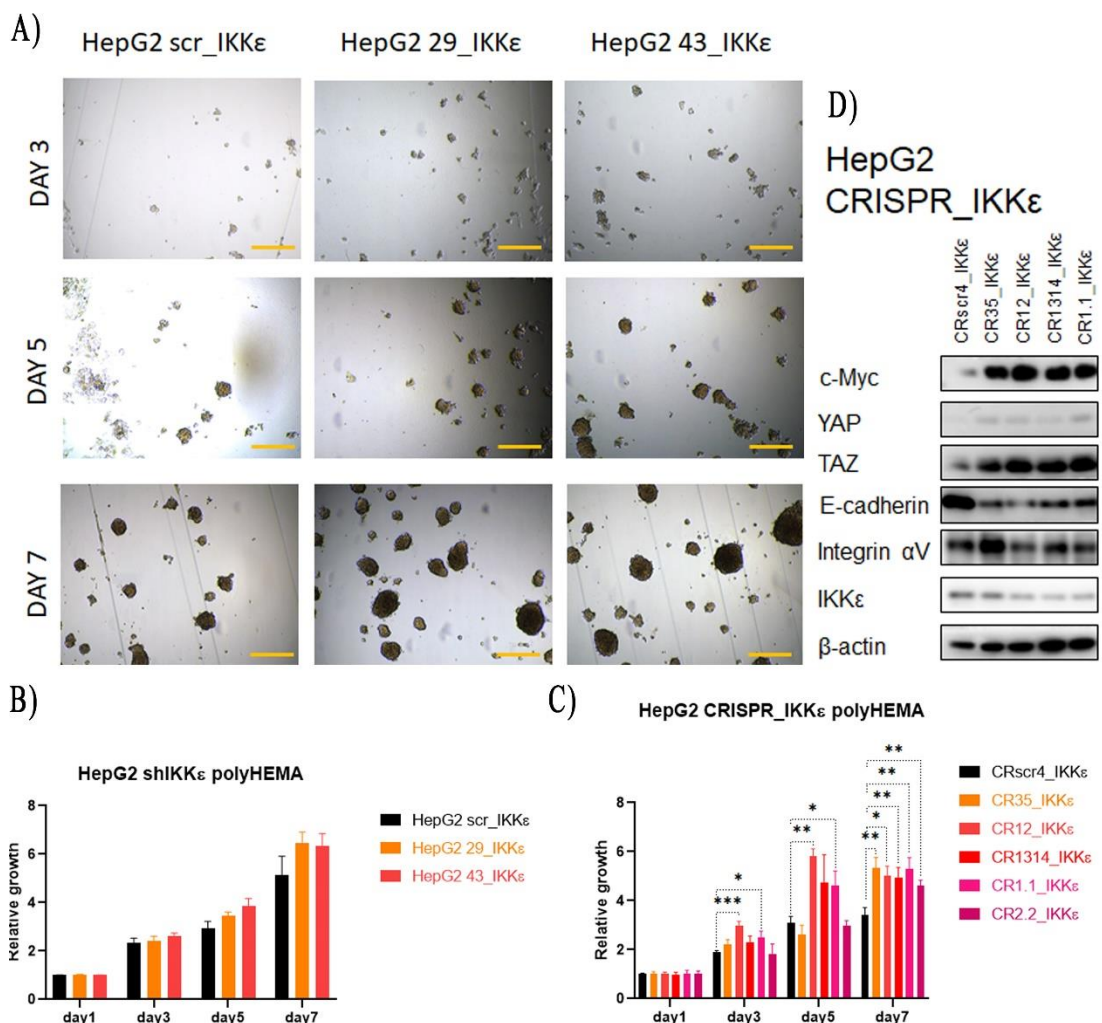


**Figure 3.2: HepG2 cells show more anchorage independence upon IKK $\epsilon$  depletion. A)** Bright-field microscopy images of control and IKK $\epsilon$ -depleted HepG2 cells growing on poly-

HEMA coated 96 well plates. **B-C)** Anchorage independent growth of IKK $\epsilon$  deficient HepG2 cells were quantified by WST-1 staining at day 1, 3, 5 and 7. Data shown are relative to each construct's day 1 value. **D)** Western blot analysis of protein markers in CRISPR/Cas9 IKK $\epsilon$  deficient HepG2 cells. Data shown are mean  $\pm$  SD of duplicate wells representative of two independent experiments; multiple t-test using Holm-Sidak method; ns not significant, \*  $p < 0.05$ , \*\*  $p < 0.01$ , \*\*\*  $p < 0.001$ , \*\*\*\*  $p < 0.0001$ . Scale bar = 300 $\mu$ m

### 3.3. EMT status of HepG2 cells shifts upon depletion or ectopic expression of IKK $\epsilon$ .

To evaluate whether IKK $\epsilon$  plays a role in EMT in HepG2 cells, IKK $\epsilon$ -depleted HepG2 cells by both shRNA and CRISPR/Cas9 methods were analysed for expression levels

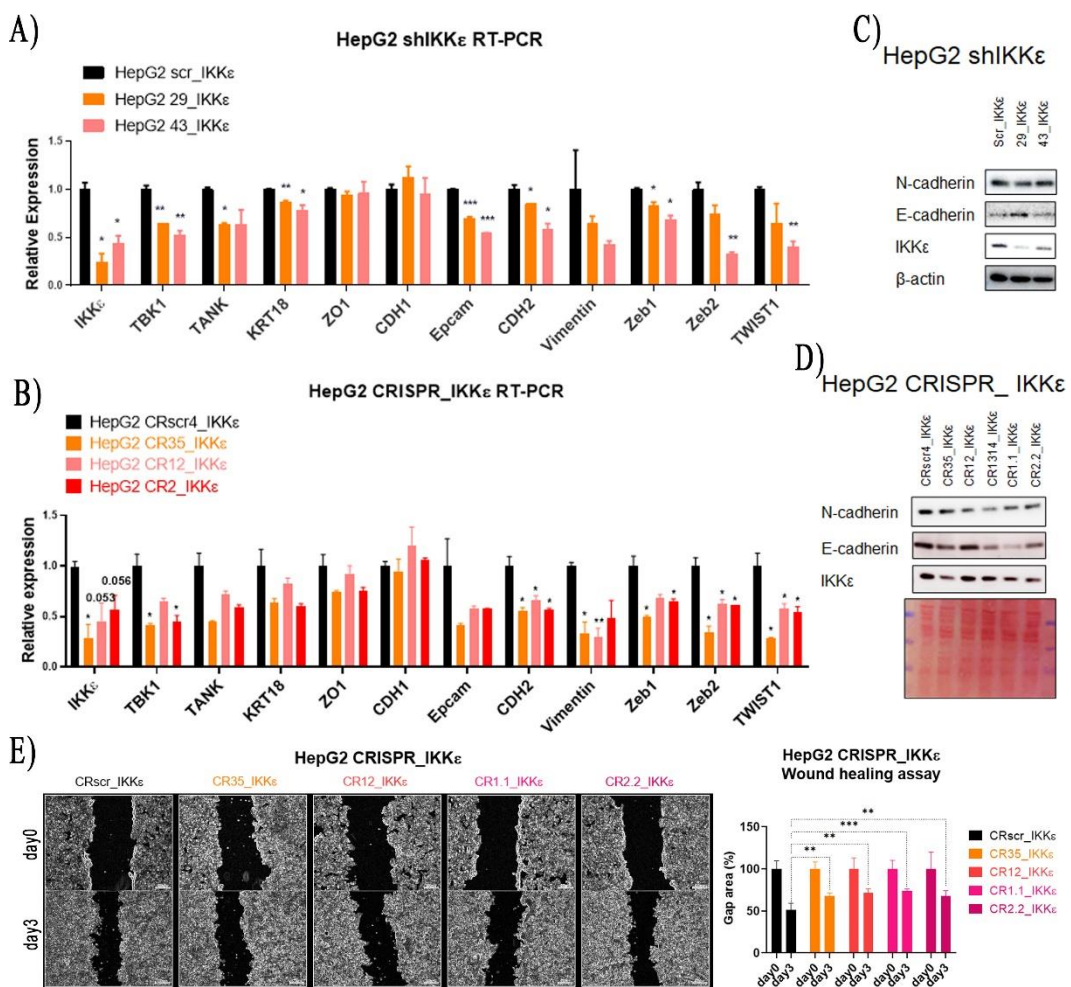


**Figure 3.3: EMT status of HepG2 cells is altered upon IKK $\epsilon$  depletion. A-B)** qPCR analysis of EMT markers in IKK $\epsilon$  depleted HepG2 cells. **C-D)** Western blot analysis of E-cadherin and

N-cadherin on IKK $\epsilon$  depleted HepG2 cells. E) Wound healing assay images of HepG2 CRISPR/Cas9 IKK $\epsilon$  depleted HepG2 cells. Quantification on the right. Data shown are mean  $\pm$  SD of triplicate wells representative of two independent experiments; t-test; ns not significant, \*  $p < 0.05$ , \*\*  $p < 0.01$ , \*\*\*  $p < 0.001$ , \*\*\*\*  $p < 0.0001$ . Scale bar = 300 $\mu$ m

of EMT markers in both RNA and protein levels (Figure 3.3. A and B). RT-PCR results of IKK $\epsilon$  depleted cells showed a significant decrease in mesenchymal markers such as CDH2, Vimentin and transcription factors Zeb1, Zeb2 and TWIST. mRNA expression of epithelial markers did not significantly change in shRNA IKK $\epsilon$  depleted HepG2 cells but there was a significant decrease in their expression in CRISPR/Cas9 IKK $\epsilon$  depleted HepG2 cells. In the protein levels, no such a significant change was observed with any constructs of shRNA IKK $\epsilon$ -depleted HepG2 cells (Figure 3.3 C).

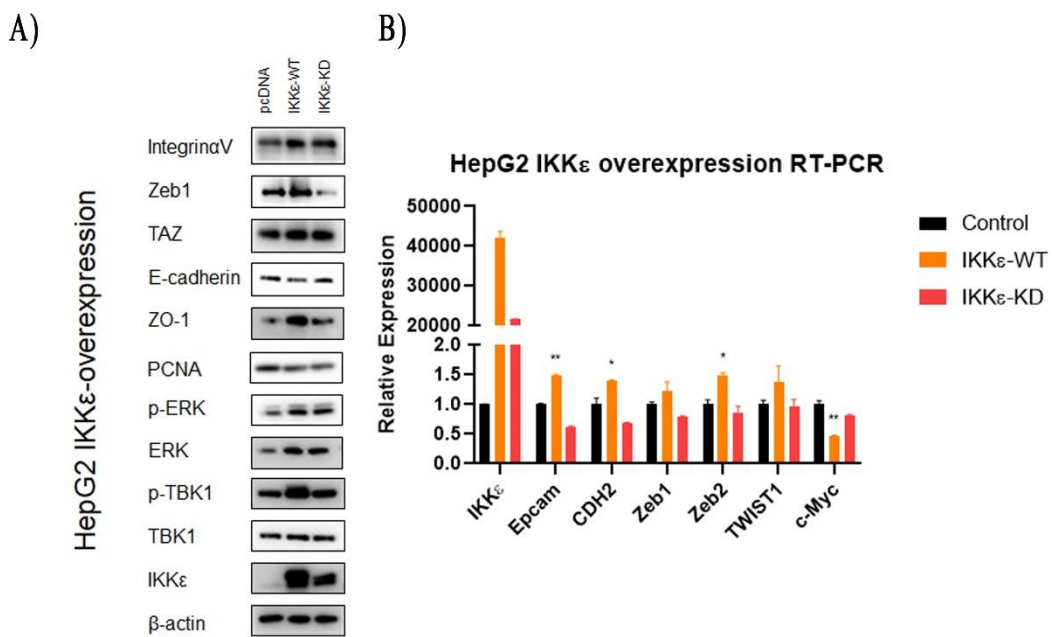


**Figure 3.4: Ectopic expression of IKK $\epsilon$  in HepG2 cells induces EMT shift. A)** Western blot analysis **B)** RT-PCR analysis of EMT markers in HepG2 cells ectopically expressing empty plasmid, IKK $\epsilon$ -WT or IKK $\epsilon$ -KD. Data shown are mean  $\pm$  SD of duplicate wells; t-test; ns not significant, \*  $p < 0.05$ , \*\*  $p < 0.01$ , \*\*\*  $p < 0.001$ , \*\*\*\*  $p < 0.0001$ .

However, in CRISPR/Cas9 IKK $\epsilon$ -depleted HepG2 cells N-cadherin is downregulated (Figure 3.3 D). Moreover, CRISPR/Cas9 IKK $\epsilon$ -depleted HepG2 cells migrate less when compared to their control cells as analysed through wound healing assay (Figure 3.3 E). Ectopic overexpression of IKK $\epsilon$  was done on HepG2 cells in order to

investigate whether the EMT status would shift in the opposite direction to IKK $\epsilon$ -depleted HepG2 cells. Expression levels of EMT markers in IKK $\epsilon$  overexpressing HepG2 cells were analysed in both protein and RNA level (Figure 3.4.). As expected, compared to control HepG2 cells, IKK $\epsilon$  overexpressing HepG2 cells harbour elevated levels of mesenchymal markers. CDH2 and Zeb2 levels are significantly upregulated in IKK $\epsilon$  overexpressing HepG2 cells. The same trend is observed for the other mesenchymal markers but the observed increase in expression is not significant (Figure 3.4 B). Protein levels of some mesenchymal markers (Integrin  $\alpha$ V, Zeb1, TAZ) are also upregulated and E-cadherin expression is downregulated upon IKK $\epsilon$  overexpression (Figure 3.4 A). Overall, we can conclude that IKK $\epsilon$  is involved in the expression of various EMT markers and has a role in maintaining the mesenchymal status of HepG2 cells.

### 3.4. TGF $\beta$ 1 induced proliferation in HepG2 cells is dependent on IKK $\epsilon$ expression.

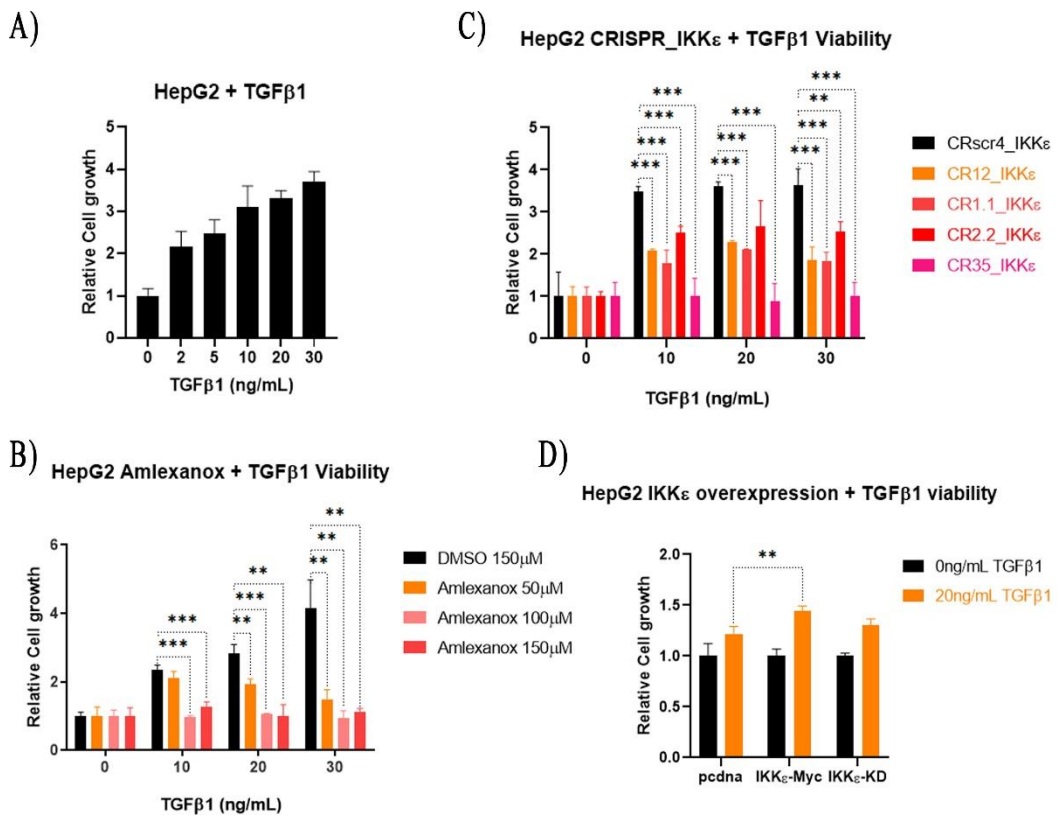


**Figure 3.5: TGF $\beta$ 1 induced proliferation in HepG2 cells is dependent on IKK $\epsilon$  expression.**

**A)** HepG2 cells, seeded in 96 well plate, were treated with different concentrations of TGF $\beta$ 1 for 72 hours. Cell viability is measured by Cell-Titer Glo Luminescent cell viability Assay. **B)**

HepG2 cells, were simultaneously treated with different doses of Amlexanox and TGF $\beta$ 1. Cell viability is measured after 72 hours of combinatory treatment using Cell-Titer Glo Luminescent cell viability Assay. Data shown are relative to each condition's 0ng/mL TGF $\beta$ 1 value. **C)** Control or CRISPR/Cas9 IKK $\epsilon$ -depleted HepG2 cells were treated for 72 hours with different concentrations of TGF $\beta$ 1. Cell viability is measured using Cell-Titer Glo Luminescent cell viability Assay. Data are shown relative to each construct's 0ng/mL TGF $\beta$ 1. **D)** Control HepG2 cells (empty vector) or HepG2 cells ectopically overexpressing IKK $\epsilon$ -WT or IKK $\epsilon$ -KD constructs were treated for 72 hours with different concentrations of TGF $\beta$ 1. Cell viability is measured using Cell-Titer Glo Luminescent cell viability Assay and data are shown relative to each construct's 0ng/mL TGF $\beta$ 1. Data are mean  $\pm$  SD of triplicate wells representative of two independent experiments; multiple t-test using Holm-Sidak method; ns not significant, \*  $p < 0.05$ , \*\*  $p < 0.01$ , \*\*\*  $p < 0.001$ , \*\*\*\*  $p < 0.0001$ .

TGF $\beta$ 1 is shown to induce EMT in HepG2 cells [63]. Considering that IKK $\epsilon$  expression levels affected EMT and proliferation of HepG2 cells, we investigated the role of IKK $\epsilon$  in TGF $\beta$ 1 signalling. HepG2 WT cells showed increased viability upon 72 hours of treatment with increasing concentrations of TGF $\beta$ 1 (Figure 3.5 A). However, TGF $\beta$ 1 induced proliferation was significantly diminished upon combinational treatment of the cells with different doses of Amlexanox, a TBK1/IKK $\epsilon$  inhibitor, and TGF $\beta$ 1 (Figure 3.5 B). A decrease in TGF $\beta$ 1 induced proliferation was also observed in CRISPR/Cas9 IKK $\epsilon$  depleted cells when compared to control cells upon treatment with different concentrations of TGF $\beta$ 1 for 72 hours (Figure 3.5 C). The opposite was observed in IKK $\epsilon$  overexpressing HepG2 cells where IKK $\epsilon$  overexpression improves cell survival upon TGF $\beta$ 1 treatment (Figure 3.5 D). Hence, IKK $\epsilon$  is important in TGF $\beta$ 1 induced proliferation in HepG2 cells.

### **3.5. IKK $\epsilon$ is involved in TGF $\beta$ 1 signalling through AKT activation.**

In order to further investigate the role of IKK $\epsilon$  in TGF $\beta$ 1 signalling, HepG2 cells were treated with 10ng/mL TGF $\beta$ 1 for short time intervals (0-4h) (Figure 3.6 A). Western blot analysis of short time TGF $\beta$ 1 treatment revealed an activation IKK $\epsilon$  (as measured by phospho-IKK $\epsilon$  WB) very early in the signalling (Figure 3.6 A). Western blot for phospho- IKK $\epsilon$  peak at 2 hours of TGF $\beta$ 1 treatment. On the other hand, 48 hours

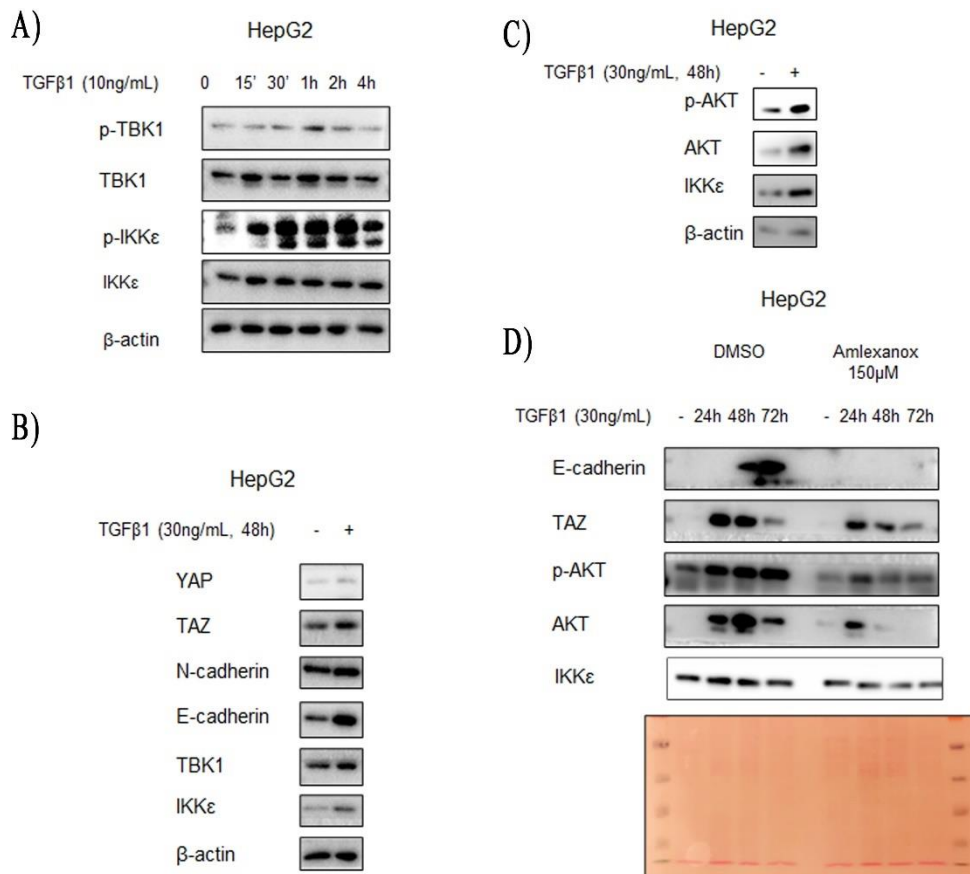


**Figure 3.6: IKKε is involved in TGFβ1 signalling through AKT activation.** **A)** Western blot analysis of HepG2 cells starved overnight and then treated with 10ng/mL TGFβ1 in different time intervals. **B-C)** Western blot analysis of HepG2 cells treated with 20ng/mL TGFβ1 for 48 hours to induce EMT and AKT activation. **C)** Western blot analysis of HepG2 cells treated simultaneously with DMSO or Amlexanox 150μM and 30ng/mL TGFβ1 for 24, 48 and 72 hours. Data are the representative of two independent experiments.

TGFβ1 (20ng/mL) treatment on HepG2 caused an upregulation of IKKε in protein level, an increased EMT and AKT activation (Figure 3.6 B and C). To specify the role of IKKε, HepG2 cells were treated with both Amlexanox and TGFβ1 (Figure 3.6 D). Western blot analysis revealed that Amlexanox treatment inhibits IKKε upregulation upon TGFβ1 treatment. Most importantly, a significant decrease in activation of AKT upon TGFβ1 treatment is observed in Amlexanox treated cells suggesting a possible role for IKKε in activating of AKT upon TGFβ1 treatment (Figure 3.6 D).

### 3.6. EGF signalling in HepG2 cells activates IKKε.

HepG2 cells express high levels of EGF and EGF signalling is shown to promote proliferation and migration [64] hence we wanted to investigate whether IKK $\epsilon$  is also involved in EGFR signalling in HepG2 cells. HepG2 cells were treated with 20ng/mL EGF for short time intervals (Figure 3.7 A). Western blot analysis of short treatment with EGF revealed an activation of IKK $\epsilon$  and upregulation of phospho- IKK $\epsilon$  levels (Figure 3.7 A) Moreover, IKK $\epsilon$  is upregulated upon 48 hours of EGF exposure (Figure 3.7 B). However, no further investigation on the involvement of IKK $\epsilon$  in EGFR signalling was performed.

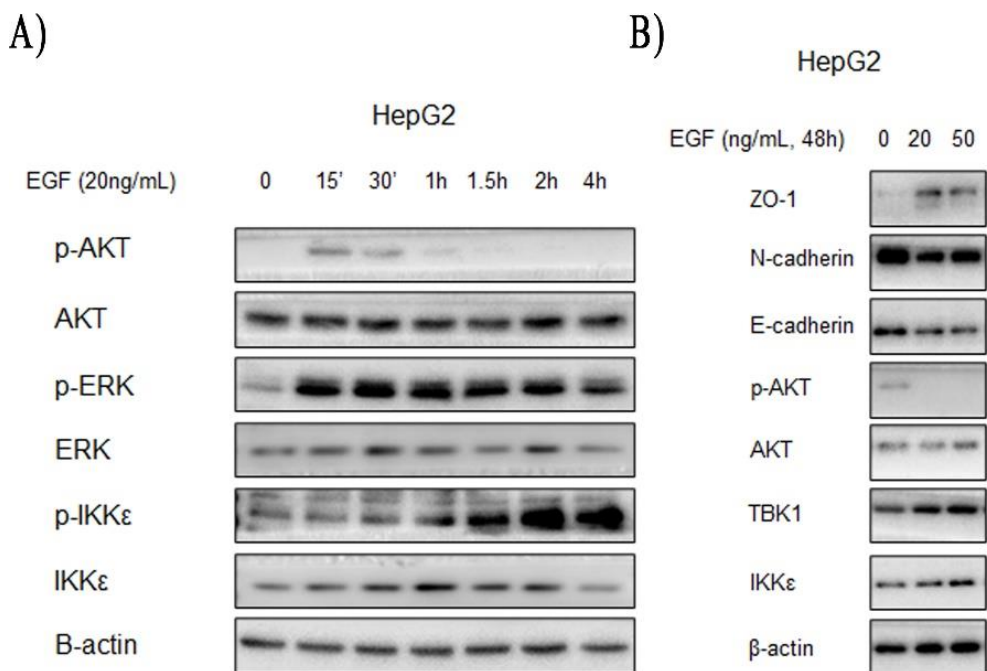


**Figure 3.7: EGFR signalling in HepG2 cells activates and upregulates IKK $\epsilon$ .** **A)** Western blot analysis of HepG2 cells starved overnight and then treated with 20ng/mL EGF in different time intervals. **B)** Western blot analysis of HepG2 cells treated with different doses of EGF for 48 hours. Data are the representative of two independent experiments.

### 3.7. Sorafenib resistance of HepG2 cells improves upon IKK $\epsilon$ depletion or pharmacological inhibition.

HCC patients receiving systemic therapy with Sorafenib develop resistance to it within 6 months [59]. Considering that IKK $\epsilon$  is involved in proliferation and EMT of HepG2

cells, we further investigated its role in Sorafenib resistance. IKK $\epsilon$  depleted HepG2 cells via shRNA (Figure 3.8. A) are more resistant to Sorafenib when compared to control cells but the difference is not significant. However, CRISPR/Cas9 IKK $\epsilon$ -depleted HepG2 cells significantly survive better harbouring a higher Sorafenib IC<sub>50</sub> than the control cells (Figure 3.8. B). The opposite is observed in IKK $\epsilon$  overexpressing HepG2 cells where Sorafenib resistance decreases compared to control cells (Figure 3.8 C) Moreover, pharmacological inhibition of IKK $\epsilon$  with Amlexanox significantly improves Sorafenib resistance of HepG2 cells in a dose dependent manner (Figure 3.8. D and E).

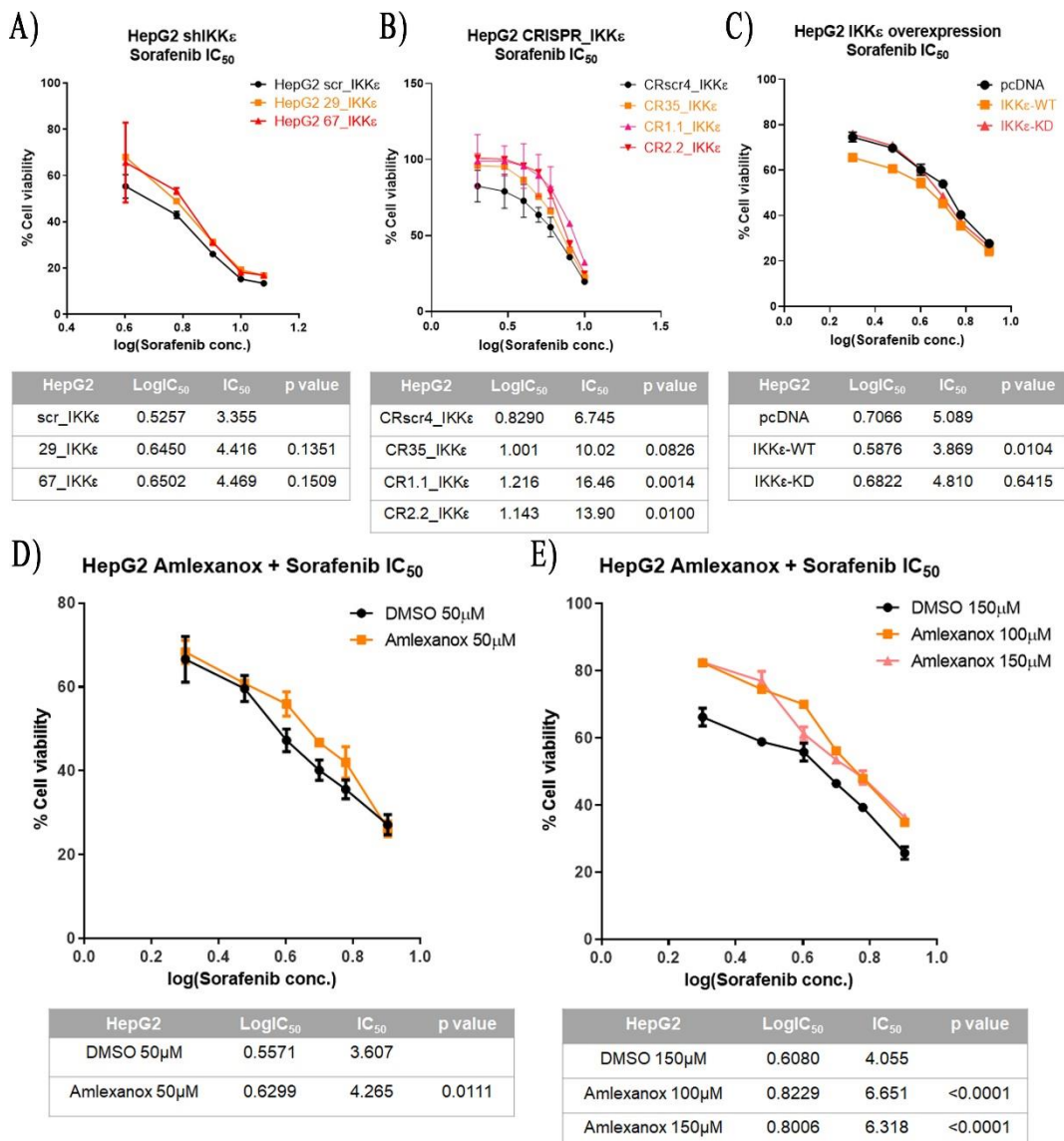


**Figure 3.8: Resistance of HepG2 cells to Sorafenib treatment improves upon IKK $\epsilon$  depletion or pharmacological inhibition. HepG2 cells with A) shRNA and B) CRISPR/Cas9 mediated IKK $\epsilon$  depletion, C) HepG2 cells overexpressing IKK $\epsilon$  and HepG2 cells treated with D)**

50 $\mu$ M Amlexanox **E**) 100 or 150 $\mu$ M Amlexanox are treated with indicated concentrations of Sorafenib for 72 hours. Cell viability is measured by Cell-Titer Glo Luminescent cell viability assay. Sorafenib IC<sub>50</sub> is analysed using GraphPad Prism 8.3.0. Data are mean  $\pm$  SD of duplicate wells representative of two independent experiments; comparison of fit of one curve fit to all data sets; ns not significant, \* p<0.05, \*\* p<0.01, \*\*\* p<0.001, \*\*\*\* p<0.0001.

### 3.8. Preparation of HepG2 Sorafenib resistant cell lines.

In order to create the Sorafenib resistant HepG2 cell line, HepG2 cells were continuously exposed to Sorafenib. The Sorafenib concentration HepG2 cells were initially exposed to is 3 $\mu$ M, a value slightly smaller than the Sorafenib IC<sub>50</sub> value of naïve HepG2 cells (3.5-4.5 $\mu$ M). HepG2 cells surviving in a specific Sorafenib concentration for 3 passages were subjected to an increase in sorafenib concentration of 0.5 $\mu$ M. This design was used to create HepG2 SORA line. In order to speed up the development of Sorafenib resistance, a different approach was used to create HepG2 SORB line where HepG2 cells were challenged to an increase of 0.5 $\mu$ M in Sorafenib concentration every other split. The maximum Sorafenib concentration cells were exposed to is the clinically relevant dose of 10 $\mu$ M [65]. A schematic representation of the approaches used to develop Sorafenib resistant HepG2 SORA and SORB lines can be found in Figure 3.9.

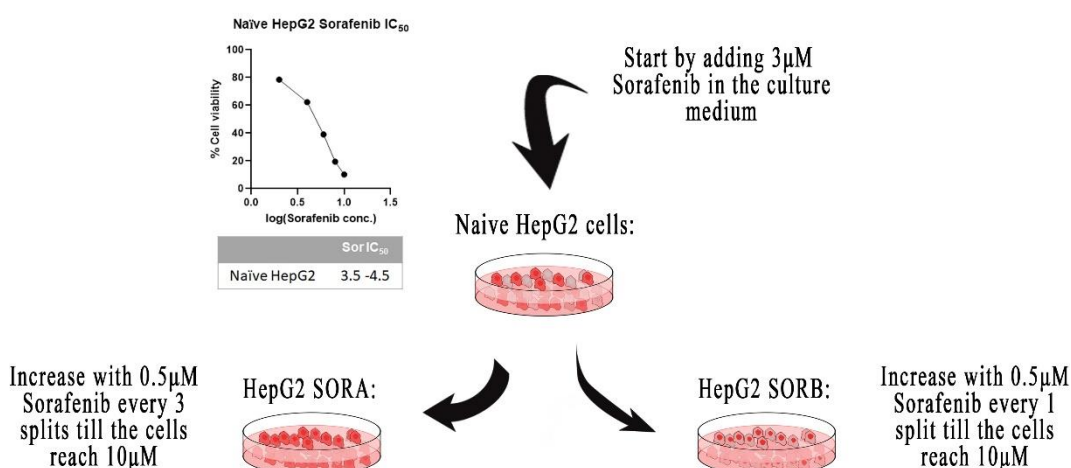


**Figure 3.9: Schematic representation of Sorafenib resistant HepG2 cell line development.** Two different approaches were used to create HepG2 SORA and SORB Sorafenib resistant cell lines.

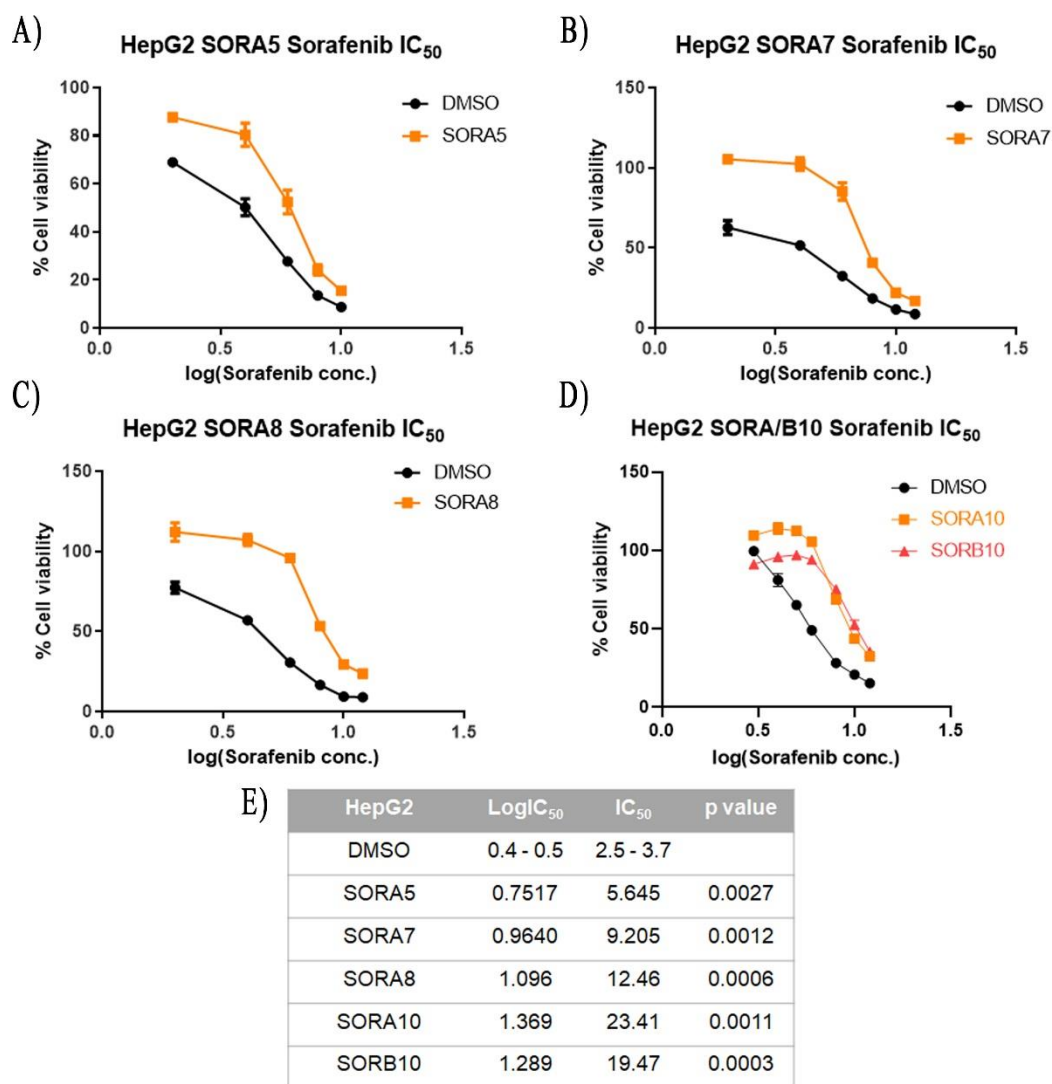


**Figure 3.10: Determination of Sorafenib IC<sub>50</sub> of HepG2 SOR cells.** Sorafenib IC<sub>50</sub> graphs of HepG2 A) SOR5 cells B) SORA7 cells. C) SORA8 cells D) SORA10 and SORB10. E) Summary table of Sorafenib IC<sub>50</sub> values of the graphs shown in A, B, C and D and corresponding p values. Data are mean ± SD of duplicate wells representative of two independent experiments; comparison of fit of one curve fit to all data sets; ns not significant, \* p<0.05, \*\* p<0.01, \*\*\* p<0.001, \*\*\*\* p<0.0001. Scale bar = 300µm.

Throughout the rest of the thesis, the number following the name of the line (ex: SORA7) will indicate the concentration of Sorafenib the cells were exposed to and are surviving in the moment a specific experiment is performed. Additionally, control cells used in the following experiments are HepG2 cells kept in DMSO concentrations same as HepG2 SOR cells. The time control cells have been exposed to DMSO is also same

as HepG2 SOR cells. There are multiple parameters that a cell line should fulfill to be considered resistant to a drug. There are multiple parameters that a cell line should

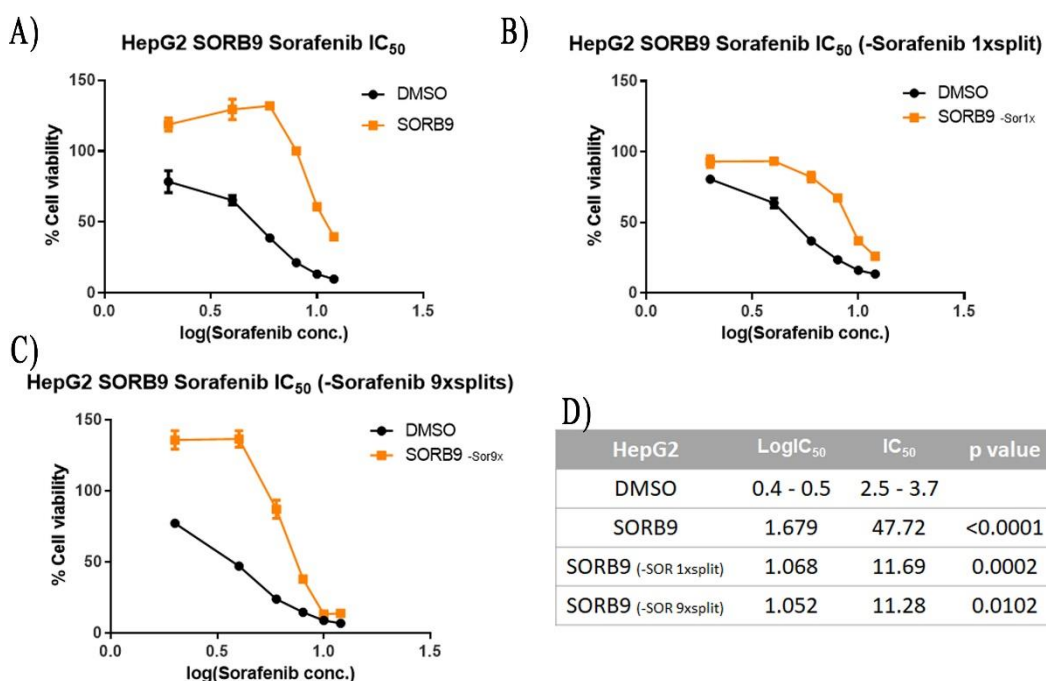


**Figure 3.11: Stability of Sorafenib IC<sub>50</sub> of HepG2 SORB9 cells upon removal of Sorafenib from culture medium.** Sorafenib IC<sub>50</sub> graph of **A)** HepG2 SORB9 cells. **B)** HepG2 SORB9 cells 1 split after Sorafenib removal, **C)** HepG2 SORB9 cells 9 splits after sorafenib removal. **D)** Summary table of Sorafenib IC<sub>50</sub> values and the corresponding p values. of the graphs shown in A, B and C. Data are mean  $\pm$  SD of duplicate wells representative of one experiment; comparison of fit of one curve fit to all data sets; ns not significant, \*  $p < 0.05$ , \*\*  $p < 0.01$ , \*\*\*  $p < 0.001$ , \*\*\*\*  $p < 0.0001$ .

fullfill to be considered resistant to a drug. For this reason, throughout the process of creating the Sorafenib resistant HepG2 cell lines, SORA and SORB, Sorafenib IC<sub>50</sub> value of the cells was analysed at vareous time surviving at 5, 7 an 8 $\mu$ M Sorafenib are shown. P values indicate a significant difference between the HepG2 SOR cells and their respective control cells (Figure 3.10 E). A 3- time increase in IC<sub>50</sub> of drug resistant cells SORB compared to their naïve counterparts is frequently required and considered to be sufficient. HepG2 SORA8 cells already reached an Sorafenib IC<sub>50</sub> 3 times higher than that of their control cells' (Figure 3.10 C and E). However, the clinically relevant dose of Sorafenib is 10 $\mu$ M. For this reason we continued to increase

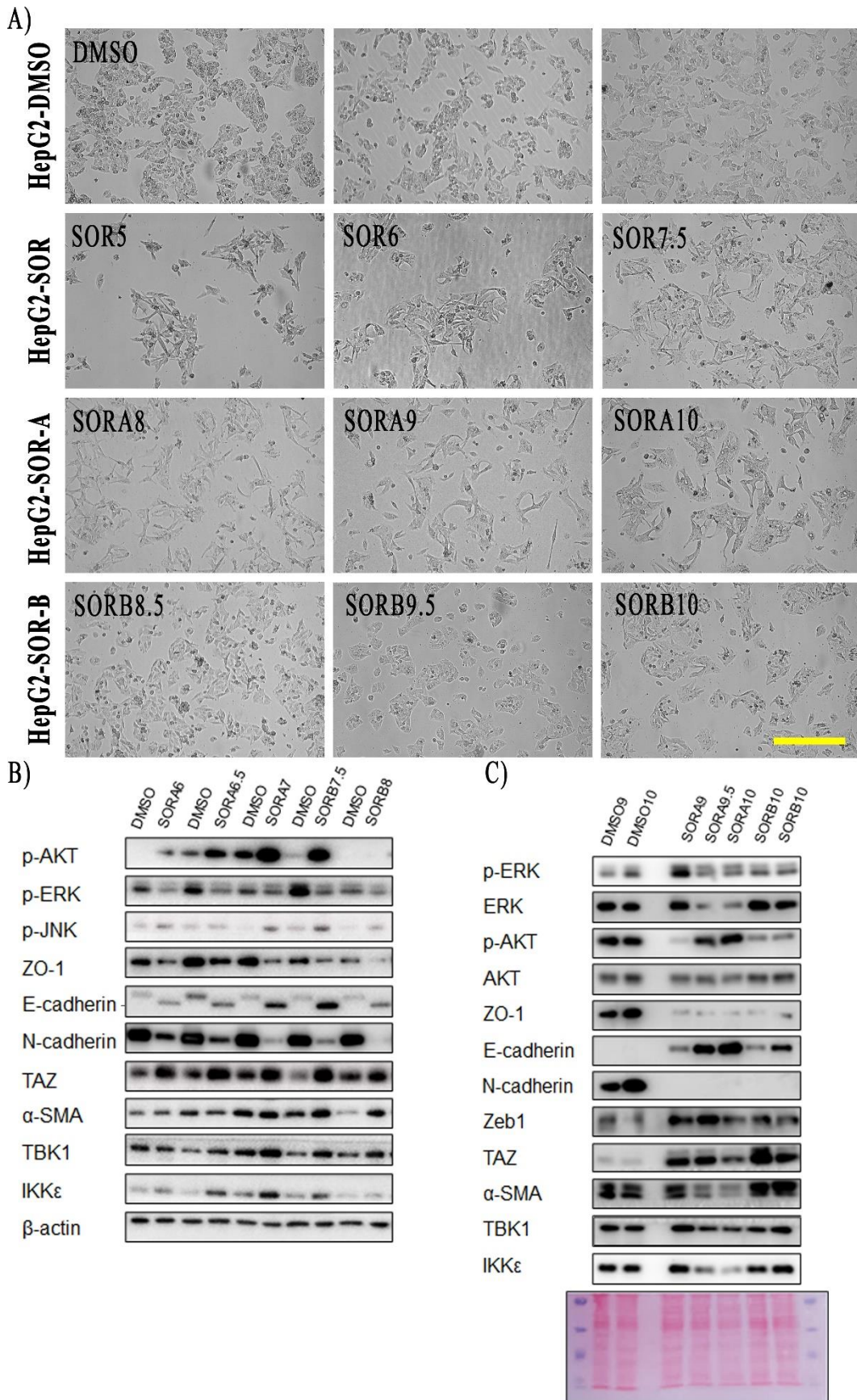


**Figure 3.12: Morphology and expression of EMT markers in HepG2 SOR cells. A)** Bright field microscopy images of control cells (top three) and HepG2 SOR cells throughout the course

of Sorafenib resistance development. Scale bar = 300 $\mu$ m **B and C)** Western blot analysis of HepG2 SOR cells.

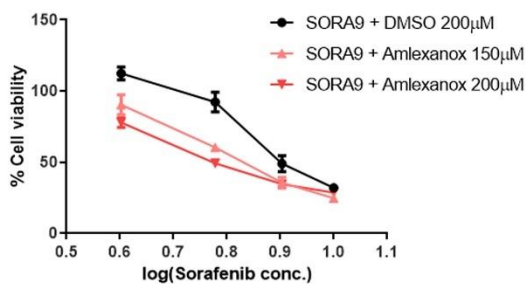
the Sorafenib concentration in their medium till 10 $\mu$ M. Sorafenib IC<sub>50</sub> of SORA10 and SORB10 is more than 3 times higher than the control cells and significantly different (Figure 3.10 D and E). In order for Sorafenib resistant cells to be used in experimental procedures, Sorafenib needs to be removed from their growth medium. Upon removal, cells should remain stable. For this reason, we checked Sorafenib IC<sub>50</sub> stability of HepG2 SOR cells upon removal of Sorafenib from their medium (Figure 3.11). Sorafenib IC<sub>50</sub> analysis was done on HepG2 SORB9 cells that were always kept in Sorafenib (Figure 3.11 A) and HepG2 SORB9 cells which were kept without Sorafenib in their medium for 1 passage (Figure 3.11 B) and 9 passages (Figure 3.11 C). Although there is a significant drop in Sorafenib IC<sub>50</sub> from cells always kept in Sorafenib to 1 split without Sorafenib, after Sorafenib removal Sorafenib IC<sub>50</sub> value remain constant for 9 passages (Figure 3.11 D). Despite the fact that Sorafenib IC<sub>50</sub> values of HepG2 SORA and SORB line are quite similar to one another and significantly higher than their control counterparts, the morphologies of the cells are not (Figure 3.12. A). SORA line cells have a very distinct morphology typical of mesenchymal cells: long bodies with extensions, cells growing separate from one another. On the other hand, morphology of SORB line is no different than the morphology of control HepG2 cells: small bodies, cells growing in groups. The fact that there is a difference in the development of resistance between the two lines could explain also the difference in morphology. Protein expression levels of some mesenchymal markers (TAZ, Zeb1,  $\alpha$ -SMA) and epithelial markers (E-cadherin, ZO-1) are also different between SORA and SORB lines (Figure 3.12 C). However, throughout the development of resistance, IKK $\epsilon$  was upregulated (Figure 3.12 B) and remains to be upregulated in SORB line (Figure 3.12 C).

### **3.9. Sorafenib resistance of HepG2 SORA/B cells reduces upon pharmacological inhibition of IKK $\epsilon$ .**

IKK $\epsilon$  was upregulated in HepG2 SORA and SORB cells at 6, 6.5, 7. 8 and 8.5 $\mu$ M Sorafenib concentrations (Figure 3.12 B) and remains to be upregulated at SORA9 and SORB10. For this reason, we wanted to investigate whether pharmacological inhibition of IKK $\epsilon$  would have an effect on the Sorafenib IC<sub>50</sub> of the HepG2 SORA

and SORB cells (Figure 3.13 B and C). HepG2 SORA9 and SORB10 treated simultaneously with Amlexanox and Sorafenib have a significantly lower IC<sub>50</sub> value than their respective controls. Hence, we can conclude that IKK $\epsilon$  may play a role in Sorafenib resistance of the HepG2 cells.

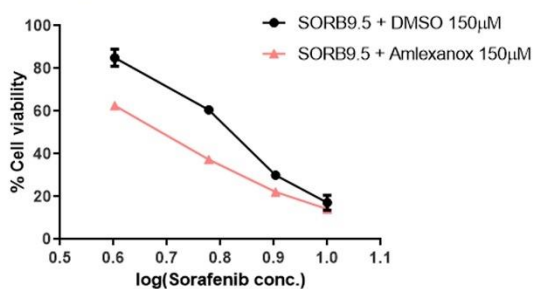
A) HepG2 SORA9 Amlexanox + Sorafenib IC<sub>50</sub>



HepG2 SORA9	LogIC <sub>50</sub>	IC <sub>50</sub>	p value
DMSO 200µM	1.165	14.62	
Amlexanox 150µM	0.8641	7.314	0.0077
Amlexanox 200µM	0.7795	6.019	<0.0001

B)

HepG2 SORB9.5 Amlexanox + Sorafenib IC<sub>50</sub>



HepG2-SORB9.5	LogIC <sub>50</sub>	IC <sub>50</sub>	P value
DMSO 150µM	0.7908	6.177	
Amlexanox 150µM	0.5466	3.520	0.0014

**Figure 3.13: IKK $\epsilon$  is important for the survival of Sorafenib resistant HepG2 cells.** Sorafenib IC<sub>50</sub> of A) SORA9 B) SORB9.5 treated simultaneously with Amlexanox at the indicated concentrations. Data are mean  $\pm$  SD of duplicate wells representative of two independent experiments; comparison of fit of one curve fit to all data sets; ns not significant, \* p<0.05, \*\* p<0.01, \*\*\* p<0.001, \*\*\*\* p<0.0001.

## CHAPTER 4

### Discussion

Hepatocellular carcinoma is the second cause of cancer-related death due to poor prognosis and lack of therapeutic options. Currently, Sorafenib is the only FDA approved systemic therapy for advanced HCC patients, however it can provide a survival advantage of only 3 months. The limiting factor remains the development of Sorafenib resistance. Hence it is necessary to shed light into the mechanisms of Sorafenib resistance and investigate new possible treatment options for advanced HCC patients.

Among molecular mechanisms involved in HCC initiation, disease progression and drug resistance, chronic inflammation plays a pivotal role. In this study we analysed the role of IKK $\epsilon$ , a non-canonical IKK-related kinase with well-known roles in inflammation as an activator of NF- $\kappa$ B and interferon signalling, in HCC development and Sorafenib resistance. Recent studies have shown IKK $\epsilon$  to be upregulated and have an oncogenic potential in many cancers including breast cancer, ovarian cancer and colorectal cancer. IKK $\epsilon$  was shown to modulate PI3K/AKT pathway, WNT signalling, Hippo pathway and NF- $\kappa$ B pathway and stimulate cancer development and progression. Better understanding of HCC development and the role of IKK $\epsilon$  can reveal new treatment opportunities for HCC patients.

In this study, HepG2 cell line is used as a model for HCC tumorigenesis. HepG2 cell line harbours mutations in NRAS, CTNNB1 ( $\beta$ -catenin) and TP53 [68]. Additionally, HepG2 cells do not contain HBV or HCV infection, common for other HCC cell lines (ex: Hep3B) and very crucial risk factor in HCC development in patients. Loss of function models, shRNA or CRISPR/Cas9, were used to study the role of IKK $\epsilon$ . IKK $\epsilon$  depletion in HepG2 cells induced an increase in proliferation as shown by the viability assays in a span of 5 days and RTCA-proliferation. Additionally, cell cycle analysis reveals that upon IKK $\epsilon$  depletion, HepG2 cell population in S-phase increases slightly and the opposite is observed in IKK $\epsilon$  overexpressing HepG2 cells. However, IKK $\epsilon$ -depletion results in a decrease in AKT

activation and IKK $\epsilon$ -overexpression induces AKT activation (as shown by phospho-AKT levels) in HepG2 cells. The role of IKK $\epsilon$  in activating AKT and directly phosphorylating it has been previously shown [50-53]. Nonetheless, the reason why upon IKK $\epsilon$  depletion and consequently less AKT activation HepG2 cells proliferate more, is not fully understood. PI3K/AKT signalling pathway is not the only pathway being regulated by IKK $\epsilon$  activity. For this reason, we can hypothesize that other pathways, being activated upon IKK $\epsilon$  depletion, induce proliferation on HepG2 cells. Downregulation of c-MYC, a very important oncogene, in mRNA level in IKK $\epsilon$  overexpressing HepG2 cells and upregulation of c-Myc and YAP/TAZ proteins in CRISPR/Cas9 IKK $\epsilon$  depleted HepG2 cells might indicate that WNT and Hippo signalling pathways are possible targets of IKK $\epsilon$  through which proliferation of HepG2 cells is regulated.

Anchorage-independent growth is a measure of cells ability to proliferate without signals from extracellular matrix (ECM), usually integrins [60]. It is crucial for tumor cells to undergo certain molecular changes, many of which epigenetic, overcome anoikis, gain anchorage-independent growing potential and metastasise to distant tissue [61]. For this reason, anchorage-independent growth is listed as one of the hallmarks of cancer. IKK $\epsilon$  depleted HepG2 cells via shRNA, only show a trend in increase of anchorage-independent growth but IKK $\epsilon$  depleted HepG2 cells via CRISPR/Cas9 method show a significant increase in anchorage-independent growth when compared to control cells. A study on pancreatic cancer concludes that depletion of integrin  $\alpha 5$  results in an increase in proliferation, motility and anchorage-independent growth of pancreatic cancer cells [62]. Similarly, IKK $\epsilon$  depleted HepG2 cells show a decrease in expression of integrin  $\alpha 5$  when compared to control cells. Hence, we can hypothesize that the decrease in expression of integrin  $\alpha 5$  seen in IKK $\epsilon$  depleted HepG2 cells contributes in the increased anchorage-independent growth of cells. Moreover, a decrease in E-cadherin expression and increase in c-Myc and TAZ expression, as observed in CRISPR/Cas9 IKK $\epsilon$  depleted HepG2, can enhance the anchorage-independent growth of the cells [60, 61, 63].

Overall, there is a significant shift in EMT upon IKK $\epsilon$  depletion. In mRNA level, both shRNA and CRISPR/Cas9 IKK $\epsilon$  depleted HepG2 cells show a significant decrease in expression of mesenchymal markers including CDH2, Vimentin, Zeb1, Zeb2 and

TWIST1 when compared to their control cells. However, N-cadherin protein levels are decreased in CRISPR/Cas9 IKK $\epsilon$  depleted cells. This shift in EMT, indicates that IKK $\epsilon$  expression is important for EMT status of the cells and for their ability to migrate, as shown by the wound healing assay. The opposite trend is observed in IKK $\epsilon$  overexpressing HepG2 cells where in mRNA level mesenchymal markers CDH2, Vimentin, Zeb1, Zeb2 and TWIST1 and in protein level TAZ, Zeb1 and integrin  $\alpha$ 5 are upregulated. Multiple times in literature, an increase in proliferation of the cells is shown to be accompanied with a decrease in EMT and vice versa [72]. Similarly, this appears to be the case in HepG2 cells where IKK $\epsilon$  depletion improves proliferation but induces a decrease in expression of mesenchymal markers and IKK $\epsilon$  overexpression impairs proliferation and induces an increase in EMT status of the cells. These results support the view that IKK $\epsilon$  might play different roles in different tumor development stages considering that high proliferation capacity is necessary for tumor initiation but a more mesenchymal state is important in invasive and metastatic potential of cancer cells [72, 73, 74, 77]. Kinases showing similar behaviour to IKK $\epsilon$  have been suggested as possible drug targets in more metastatic stages of tumor development [74, 75]

The EMT shift upon IKK $\epsilon$  depletion is the first indicator that IKK $\epsilon$  might play a role in EMT status of HepG2 cells. Previous studies have shown TGF $\beta$ 1 to induce EMT and promote migration and invasion in HepG2 cells [63]. Additionally, HepG2 cell line was shown to not be affected by the cytostatic effect of TGF $\beta$ 1 [70]. HepG2 cells in our hand proliferate more than control cells upon TGF $\beta$ 1 treatment. Additionally, TGF $\beta$ 1 induced proliferation in HepG2 cells diminishes upon pharmacological inhibition of IKK $\epsilon$  with Amlexanox or depletion of IKK $\epsilon$  via CRISPR/Cas9. Opposite to these results, TGF $\beta$ 1 induced proliferation improves upon IKK $\epsilon$  overexpression in HepG2 cells. Moreover, western blot analysis reveals that IKK $\epsilon$  is downstream of TGF $\beta$ 1, activated by short time treatment with TGF $\beta$ 1 and upregulated in 48-hour treatment with TGF $\beta$ 1. Activation of IKK $\epsilon$  upon TGF $\beta$ 1 appears to be important for AKT phosphorylation and upregulation. TGF $\beta$ 1 signalling has been shown to activate PI3K/AKT signalling pathway [66], but AKT activation in TGF $\beta$ 1 treated HepG2 cells diminishes upon IKK $\epsilon$  pharmacological inhibition. Moreover, E-cadherin and TAZ, shown to be upregulated upon TGF $\beta$ 1 signalling are not upregulated at the same level upon pharmacological inhibition of IKK $\epsilon$  indicating that their regulation is

downstream of IKK $\epsilon$ . IKK $\epsilon$ 's involvement in TGF $\beta$ 1 signalling is additional proof of the importance of IKK $\epsilon$  in EMT status of the cells.

EGF signalling has also been shown previously to promote proliferation and migration of HepG2 cells [64]. EGF treatment in HepG2 cells reveals that IKK $\epsilon$  is downstream of EGFR, activated early in the signalling and upregulated in protein level upon 48-hour EGF treatment. Further analysis on the specific role of IKK $\epsilon$  in EGFR signalling were not performed, but considering the role of IKK $\epsilon$  in EMT and proliferation, a possible role in EGF-induced EMT can be hypothesized. Moreover, IKK $\epsilon$  was shown to be activated only by the mutated EGFR in NSLC [40]. However, HepG2 cells do not harbour mutations in EGFR [68, 69]. Hence, activation of IKK $\epsilon$  upon EGFR signalling in HCC might be independent of the mutation status of EGFR.

Development of Sorafenib resistance in HCC patients is a complex process. However, one of the mechanisms involved in drug resistance development is EMT. Enhanced mesenchymal markers and migratory/invasive potential and reduced epithelial markers are directly related to drug resistance in general, including Sorafenib resistance [72]. In naïve HepG2 cells, IKK $\epsilon$  depletion improves proliferation of HepG2 cells. The involvement of IKK $\epsilon$  in proliferation of naïve HepG2 cells is also reflected in the ability of the cells to withstand slightly higher doses of Sorafenib, as shown by the increase in Sorafenib IC<sub>50</sub> in IKK $\epsilon$  depleted HepG2 cells. The opposite is observed in IKK $\epsilon$  overexpressing HepG2 cells where IKK $\epsilon$  overexpression increases the sensitivity of naïve HepG2 cells to Sorafenib. YAP/TAZ upregulation has been previously linked to the increase in proliferation and chemoresistance of cancer cells [78] Similarly, YAP/TAZ upregulation in IKK $\epsilon$  depleted HepG2 cells might be the underlying reason promoting proliferation and resistance to Sorafenib at the same time.

In Sorafenib resistant HepG2 cells, IKK $\epsilon$  appears to be upregulated. The reasons behind the upregulation of IKK $\epsilon$  in Sorafenib resistant HepG2 cells remain to be further investigated. However, considering that IKK $\epsilon$  overexpression induces an increase in expression of mesenchymal markers, we can hypothesize that the upregulation of IKK $\epsilon$  is necessary for Sorafenib resistant HepG2 cells to achieve an EMT shift to a more mesenchymal state. At the same time, the presented results on naïve HepG2 cells overexpressing IKK $\epsilon$  and Sorafenib resistant HepG2 cells where

IKK $\epsilon$  is upregulated are consistent with clinicopathological studies showing that most of the circulating tumor cells in the blood, hence the cells with the highest potential to metastasise, have decreased proliferation potential but high resistance to chemotherapy and a mesenchymal phenotype [73]. For this reason, pharmacological inhibition of IKK $\epsilon$  sensitizes the Sorafenib resistant HepG2 cells to Sorafenib. However, we should also consider the fact that Sorafenib resistant HepG2 cells used in this study, despite the fact that their resistance to Sorafenib was significantly higher than the control cells and morphology of HepG2 SORA line is very mesenchymal-like, did not have a full EMT shift. E-cadherin is upregulated and N-cadherin is downregulated in Sorafenib resistant HepG2 cells. Hence, it remains to be studied whether IKK $\epsilon$  will continue to be upregulated in a case where Sorafenib resistant HepG2 cells will exhibit the EMT profile of fully drug resistant cells.

## CHAPTER 5

### Conclusion and Future Perspective

In this study, the roles of IKK $\epsilon$  in hepatocellular tumorigenesis are examined. Other studies in different cancer types including breast cancer, ovarian cancer and prostate cancer have shown IKK $\epsilon$  to be overexpressed and act as an oncogene. However, in HCC this does not appear to be always the case. In naïve HepG2 cells, IKK $\epsilon$  depletion improves proliferation and increases anchorage-independent growth of HepG2 cells. Moreover, IKK $\epsilon$  depletion or pharmacological inhibition increases the resistance of HepG2 cells to short term Sorafenib treatment. Hence, IKK $\epsilon$  appears to play tumor suppressive roles in tumor initiation stages. However, at the same time, IKK $\epsilon$  depletion is related to a decrease in expression of mesenchymal markers and IKK $\epsilon$  expression is involved in TGF $\beta$ 1 signalling and TGF $\beta$ 1 induced proliferation and EMT in HepG2 cells. These results closely relate IKK $\epsilon$  expression to EMT status of the cells. Moreover, IKK $\epsilon$  is upregulated in Sorafenib resistant HepG2 cells. Pharmacological inhibition of IKK $\epsilon$  in Sorafenib resistant HepG2 cells sensitises the cells to Sorafenib showing an oncogenic potential of IKK $\epsilon$  in later stages of tumor progression such as metastasis and drug resistance. Hence, IKK $\epsilon$  appears to be involved in multiple different pathways regulating proliferation, EMT and drug resistance but whether it is an oncogene or tumor suppressor depends on the context it is being studied and different stages of tumor formation and progression.

There are multiple aspects that need to be considered and further studied in order to finalize the role of IKK $\epsilon$  in HCC tumorigenesis. First, IKK $\epsilon$  is an inducible kinase and its expression levels might be dependent on multiple signalling and stimuli in HCC. For this reason, better understanding on the regulation of expression of IKK $\epsilon$  in epigenetic level would shed more light on the roles of IKK $\epsilon$  in tumorigenesis. Moreover, there exist some redundancy between IKK $\epsilon$  and the kinase most closely related to it, TBK1. In our settings, IKK $\epsilon$  depletion via shRNA or CRISPR/Cas9 method causes some change in expression of TBK1 as well and Amlexanox is a dual inhibitor of IKK $\epsilon$  and TBK1. Hence, better targeting of IKK $\epsilon$ , without effecting TBK1 expression and activity, would provide for results with higher specificity.

Additionally, the results presented in this study are based solely on *in vitro* experimentation. It is necessary to analyse IKK $\epsilon$  in *in vivo* settings due to the fact that IKK $\epsilon$  is an inflammation-related kinase. In tumor microenvironment, there are multiple factors, including cytokines, growth factors and tumor infiltrating immune cells that might be able to affect IKK $\epsilon$  expression and activity. Hence, further *in vivo* work on the roles of IKK $\epsilon$  in HCC tumorigenesis would complement the *in vitro* conclusions suggested by this study. Lastly, we should keep in mind that the results are based on HepG2 cell line. The genetic background of HepG2 cells might not be representative of all HCC patients and it would be beneficial to show that same mechanisms are true in other HCC cell lines as well.

Further study on the mechanisms of Sorafenib resistance is necessary in order to develop new treatment options for advanced HCC patients. Results presented in this study implicate IKK $\epsilon$  in the development of Sorafenib resistance. The use of Amlexanox, the pharmacological inhibitor of IKK $\epsilon$ , in Sorafenib resistant HepG2 cells results in an inhibition of proliferation, decrease in viability and further sensitizes the cells to Sorafenib. However, the mechanisms behind the role of IKK $\epsilon$  in Sorafenib resistance needs further investigation and in-depth analysis of the development of Sorafenib resistance would benefit advanced HCC patients progressing on Sorafenib.

## Bibliography

1. Bray F, Ferlay J, Soerjomataram I, et al. (2018) Global cancer statistics GLOBOCAN estimates of incidence and mortality worldwide for 36 cancers in 185 countries. *CA Cancer J Clin.* 2018; 68: 394- 424.
2. El-Serag, H. B., & Rudolph, K. L. (2007). Hepatocellular carcinoma: epidemiology and molecular carcinogenesis. *Gastroenterology*, 132(7), 2557–2576. doi.org/10.1053/j.gastro.2007.04.061
3. Llovet, J. M., Zucman-Rossi, J., Pikarsky, E., Sangro, B., Schwartz, M., Sherman, M., & Gores, G. (2016). Hepatocellular carcinoma. *Nature Reviews Disease Primers*, 2(1). doi: 10.1038/nrdp.2016.18
4. Forner, A., Reig, M., & Bruix, J. (2018). Hepatocellular carcinoma. *The Lancet*, 391(10127), 1301–1314. doi: 10.1016/s0140-6736(18)30010-2
5. Balogh, J., Victor, D., 3rd, Asham, E. H., Burroughs, S. G., Boktour, M., Saharia, A., Li, X., Ghobrial, R. M., & Monsour, H. P., Jr (2016). Hepatocellular carcinoma: a review. *Journal of hepatocellular carcinoma*, 3, 41–53. [doi.org/10.2147/JHC.S61146](https://doi.org/10.2147/JHC.S61146)
6. Cha, C., & Dematteo, R. P. (2005). Molecular mechanisms in hepatocellular carcinoma development. *Best practice & research. Clinical gastroenterology*, 19(1), 25–37. [doi.org/10.1016/j.bpg.2004.11.005](https://doi.org/10.1016/j.bpg.2004.11.005)
7. Llovet, J. M., Villanueva, A., Lachenmayer, A., & Finn, R. S. (2015). Advances in targeted therapies for hepatocellular carcinoma in the genomic era. *Nature reviews. Clinical oncology*, 12(7), 408–424. doi.org/10.1038/nrclinonc.2015.103
8. Raoul, J.-L., Kudo, M., Finn, R. S., Edeline, J., Reig, M., & Galle, P. R. (2018). Systemic therapy for intermediate and advanced hepatocellular carcinoma: Sorafenib and beyond. *Cancer Treatment Reviews*, 68, 16–24. doi: 10.1016/j.ctrv.2018.05.006
9. da Motta Girardi, D., Correa, T. S., Crosara Teixeira, M., & Dos Santos Fernandes, G. (2018). Hepatocellular Carcinoma: Review of Targeted and Immune Therapies. *Journal of gastrointestinal cancer*, 49(3), 227–236. doi.org/10.1007/s12029-018-0121-4
10. Keating G. M. (2017). Sorafenib: A Review in Hepatocellular Carcinoma. *Targeted oncology*, 12(2), 243–253. doi.org/10.1007/s11523-017-0484-7

11. Zhu, Y. J., Zheng, B., Wang, H. Y., & Chen, L. (2017). New knowledge of the mechanisms of sorafenib resistance in liver cancer. *Acta pharmacologica Sinica*, 38(5), 614–622. doi.org/10.1038/aps.2017.5
12. Niu, L., Liu, L., Yang, S., Ren, J., Lai, P., & Chen, G. G. (2017). New insights into sorafenib resistance in hepatocellular carcinoma: Responsible mechanisms and promising strategies. *Biochimica et biophysica acta. Reviews on cancer*, 1868(2), 564–570. doi.org/10.1016/j.bbcan.2017.10.002
13. Chen, J., Jin, R., Zhao, J., Liu, J., Ying, H., Yan, H., ... Cai, X. (2015). Potential molecular, cellular and microenvironmental mechanism of sorafenib resistance in hepatocellular carcinoma. *Cancer Letters*, 367(1), 1–11. doi: 10.1016/j.canlet.2015.06.019
14. Verhelst, K., Verstrepen, L., Carpentier, I., & Beyaert, R. (2013). I $\kappa$ B kinase  $\epsilon$  (IKK $\epsilon$ ): A therapeutic target in inflammation and cancer. *Biochemical Pharmacology*, 85(7), 873–880. doi: 10.1016/j.bcp.2013.01.007
15. Clément, J.-F., Meloche, S., & Servant, M. J. (2008). The IKK-related kinases: from innate immunity to oncogenesis. *Cell Research*, 18(9), 889–899. doi: 10.1038/cr.2008.273
16. Chau, T.-L., Gioia, R., Gatot, J.-S., Patrascu, F., Carpentier, I., Chapelle, J.-P., ... Chariot, A. (2008). Are the IKKs and IKK-related kinases TBK1 and IKK- $\epsilon$  similarly activated? *Trends in Biochemical Sciences*, 33(4), 171–180. doi: 10.1016/j.tibs.2008.01.002
17. Yin, M., Wang, X., & Lu, J. (2019). Advances in IKBKE as a potential target for cancer therapy. *Cancer Medicine*, 9(1), 247–258. doi: 10.1002/cam4.2678
18. Shimada, T., Kawai, T., Takeda, K., Matsumoto, M., Inoue, J.-I., Tatsumi, Y., ... Akira, S. (1999). IKK-i, a novel lipopolysaccharide-inducible kinase that is related to I $\kappa$ B kinases. *International Immunology*, 11(8), 1357–1362. doi: 10.1093/intimm/11.8.1357
19. Peters, R. T., Liao, S.-M., & Maniatis, T. (2000). IKK $\epsilon$  Is Part of a Novel PMA-Inducible I $\kappa$ B Kinase Complex. *Molecular Cell*, 5(3), 513–522. doi: 10.1016/s1097-2765(00)80445-1
20. Shen, R. R., & Hahn, W. C. (2010). Emerging roles for the non-canonical IKKs in cancer. *Oncogene*, 30(6), 631–641. doi: 10.1038/onc.2010.493

21. Zhang, J., Tian, M., Xia, Z., & Feng, P. (2016). Roles of I $\kappa$ B kinase  $\epsilon$  in the innate immune defense and beyond. *Virologica Sinica*, 31(6), 457–465. doi: 10.1007/s12250-016-3898-y
22. Kravchenko, V. V., Mathison, J. C., Schwamborn, K., Mercurio, F., & Ulevitch, R. J. (2003). IKKi/IKK $\epsilon$  Plays a Key Role in Integrating Signals Induced by Pro-inflammatory Stimuli. *Journal of Biological Chemistry*, 278(29), 26612–26619. doi: 10.1074/jbc.m303001200
23. Clark, K., Peggie, M., Plater, L., Sorcek, R. J., Young, E. R. R., Madwed, J. B., ... Cohen, P. (2011). Novel cross-talk within the IKK family controls innate immunity. *Biochemical Journal*, 434(1), 93–104. doi: 10.1042/bj20101701
24. Eddy, S. F., Guo, S., Demicco, E. G., Romieu-Mourez, R., Landesman-Bollag, E., Seldin, D. C., & Sonenshein, G. E. (2005). Inducible I $\kappa$ B Kinase/I $\kappa$ B Kinase  $\epsilon$  Expression Is Induced by CK2 and Promotes Aberrant Nuclear Factor- $\kappa$ B Activation in Breast Cancer Cells. *Cancer Research*, 65(24), 11375–11383. doi: 10.1158/0008-5472.can-05-1602
25. Boehm, J. S., Zhao, J. J., Yao, J., Kim, S. Y., Firestein, R., Dunn, I. F., ... Hahn, W. C. (2007). Integrative Genomic Approaches Identify IKBKE as a Breast Cancer Oncogene. *Cell*, 129(6), 1065–1079. doi: 10.1016/j.cell.2007.03.052
26. Qin, B., & Cheng, K. (2010). Silencing of the IKK $\epsilon$  gene by siRNA inhibits invasiveness and growth of breast cancer cells. *Breast Cancer Research*, 12(5). doi: 10.1186/bcr2644
27. Guan, H., Zhang, H., Cai, J., Wu, J., Yuan, J., Li, J., ... Li, M. (2010). IKBKE is over-expressed in glioma and contributes to resistance of glioma cells to apoptosis via activating NF- $\kappa$ B. *The Journal of Pathology*, 223(3), 436–445. doi: 10.1002/path.2815
28. Huang, Q. (2012). Silencing of IKK $\epsilon$  using siRNA inhibits proliferation and invasion of glioma cells in vitro and in vivo. *International Journal of Oncology*. doi: 10.3892/ijo.2012.1452
29. Kang, M. R., Kim, M. S., Kim, S. S., Ahn, C. H., Yoo, N. J., & Lee, S. H. (2009). NF- $\kappa$ B signalling proteins p50/p105, p52/p100, RelA, and IKK $\epsilon$  are over-expressed in oesophageal squamous cell carcinomas. *Pathology*, 41(7), 622–625. doi: 10.3109/00313020903257756

30. Lee, S. E., Hong, M., Cho, J., Lee, J., & Kim, K.-M. (2016). IKK $\epsilon$  and TBK1 expression in gastric cancer. *Oncotarget*, 8(10), 16233–16242. doi: 10.18632/oncotarget.9069
31. Geng, B., Zhang, C., Wang, C., Che, Y., Mu, X., Pan, J., ... You, Q. (2017). I $\kappa$ B-kinase- $\epsilon$  in the tumor microenvironment is essential for the progression of gastric cancer. *Oncotarget*, 8(43), 75298–75307. doi: 10.18632/oncotarget.20778
32. Cheng, A., Guo, J., Henderson-Jackson, E., Kim, D., Malafa, M., & Coppola, D. (2011). I $\kappa$ B Kinase  $\epsilon$  expression in pancreatic ductal adenocarcinoma. *American Journal of Clinical Pathology*, 136, 1, 60-6.
33. Zubair, H., Azim, S., Srivastava, S. K., Ahmad, A., Bhardwaj, A., Khan, M. A., ... Singh, A. P. (2016). Glucose Metabolism Reprogrammed by Overexpression of IKK $\epsilon$  Promotes Pancreatic Tumor Growth. *Cancer Research*, 76(24), 7254–7264. doi: 10.1158/0008-5472.can-16-1666
34. Goktuna, S. I., Shostak, K., Chau, T.-L., Heukamp, L. C., Hennuy, B., Duong, H.-Q., ... Chariot, A. (2016). The Prosurvival IKK-Related Kinase IKK Integrates LPS and IL17A Signaling Cascades to Promote Wnt-Dependent Tumor Development in the Intestine. *Cancer Research*, 76(9), 2587–2599. doi: 10.1158/0008-5472.can-15-1473
35. Chen, J., Zhao, J., Chen, X., Ding, C., Lee, K., Jia, Z., ... Peng, J. (2017). Hyper activation of  $\beta$ -catenin signalling induced by IKK $\epsilon$  inhibition thwarts colorectal cancer cell proliferation. *Cell Proliferation*, 50(4). doi: 10.1111/cpr.12350
36. Guo, J.-P., Shu, S.-K., He, L., Lee, Y.-C., Kruk, P. A., Grenman, S., ... Cheng, J. Q. (2009). Deregulation of IKBKE Is Associated with Tumor Progression, Poor Prognosis, and Cisplatin Resistance in Ovarian Cancer. *The American Journal of Pathology*, 175(1), 324–333. doi: 10.2353/ajpath.2009.080767
37. Hsu, S., Kim, M., Hernandez, L., Grajales, V., Noonan, A., Anver, M., ... Annunziata, C. M. (2012). IKK- $\epsilon$  Coordinates Invasion and Metastasis of Ovarian Cancer. *Cancer Research*, 72(21), 5494–5504. doi: 10.1158/0008-5472.can-11-3993
38. Hildebrandt, M. A., Tan, W., Tamboli, P., Huang, M., Ye, Y., Lin, J., ... Wu, X. (2012). Kinome expression profiling identifies IKBKE as a predictor of overall survival in clear cell renal cell carcinoma patients. *Carcinogenesis*, 33(4), 799–803. doi: 10.1093/carcin/bgs018

39. Guo, J., Kim, D., Gao, J., Kurtyka, C., Chen, H., Yu, C., ... Cheng, J. Q. (2012). IKBKE is induced by STAT3 and tobacco carcinogen and determines chemosensitivity in non-small cell lung cancer. *Oncogene*, 32(2), 151–159. doi: 10.1038/onc.2012.39
40. Challa, S., Guo, J.-P., Ding, X., Xu, C.-X., Li, Y., Kim, D., ... Cheng, J. Q. (2016). IKBKE Is a Substrate of EGFR and a Therapeutic Target in Non-Small Cell Lung Cancer with Activating Mutations of EGFR. *Cancer Research*, 76(15), 4418–4429. doi: 10.1158/0008-5472.can-16-0069
41. Lv, H. (2015). IKBKE Upregulation is Positively Associated with Squamous Cell Carcinoma of the Lung In Vivo and Malignant Transformation of Human Bronchial Epithelial Cells In Vitro. *Medical Science Monitor*, 21, 1577–1586. doi: 10.12659/msm.893815
42. Tang, D., Sun, B., Yu, H., Yang, Z., & Zhu, L. (2015). Tumor-Suppressing Effect of MiR-4458 on Human Hepatocellular Carcinoma. *Cellular Physiology and Biochemistry*, 35(5), 1797–1807. doi: 10.1159/000373991
43. Park, M., & Hong, J. (2016). Roles of NF- $\kappa$ B in Cancer and Inflammatory Diseases and Their Therapeutic Approaches. *Cells*, 5(2), 15. doi: 10.3390/cells5020015
44. Xia, Y., Shen, S., & Verma, I. M. (2014). NF-  $\kappa$ B, an Active Player in Human Cancers. *Cancer Immunology Research*, 2(9), 823–830. doi: 10.1158/2326-6066.cir-14-0112
45. Xia, L., Tan, S., Zhou, Y., Lin, J., Wang, H., Oyang, L., Tian, Y., Liu, L., Su, M., Wang, H., Cao, D., & Liao, Q. (2018). Role of the NF $\kappa$ B-signaling pathway in cancer. *OncoTargets and therapy*, 11, 2063–2073. [doi.org/10.2147/OTT.S161109](https://doi.org/10.2147/OTT.S161109)
46. Shen, R. R., Zhou, A. Y., Kim, E., Lim, E., Habelhah, H., & Hahn, W. C. (2012). I $\kappa$ B kinase  $\epsilon$  phosphorylates TRAF2 to promote mammary epithelial cell transformation. *Molecular and cellular biology*, 32(23), 4756–4768. doi.org/10.1128/MCB.00468-12
47. Hutti, J. E., Shen, R. R., Abbott, D. W., Zhou, A. Y., Sprott, K. M., Asara, J. M., ... Cantley, L. C. (2009). Phosphorylation of the Tumor Suppressor CYLD by the Breast Cancer Oncogene IKK $\epsilon$  Promotes Cell Transformation. *Molecular Cell*, 34(4), 461–472. doi: 10.1016/j.molcel.2009.04.031
48. Janku, F., Yap, T. A., & Meric-Bernstam, F. (2018). Targeting the PI3K pathway in cancer: are we making headway? *Nature Reviews Clinical Oncology*, 15(5), 273–291. doi: 10.1038/nrclinonc.2018.28

49. Noorolyai, S., Shajari, N., Baghbani, E., Sadreddini, S., & Baradaran, B. (2019). The relation between PI3K/AKT signalling pathway and cancer. *Gene*, 698, 120–128. doi: 10.1016/j.gene.2019.02.076
50. Xie, X., Zhang, D., Zhao, B., Lu, M. K., You, M., Condorelli, G., Wang, C. Y., & Guan, K. L. (2011). I $\kappa$ B kinase epsilon and TANK-binding kinase 1 activate AKT by direct phosphorylation. *Proceedings of the National Academy of Sciences of the United States of America*, 108(16), 6474–6479. doi.org/10.1073/pnas.1016132108
51. Rajurkar, M., Dang, K., Fernandez-Barrena, M. G., Liu, X., Fernandez-Zapico, M. E., Lewis, B. C., & Mao, J. (2017). I $\kappa$ BKE Is Required during KRAS-Induced Pancreatic Tumorigenesis. *Cancer Research*, 77(2), 320–329. doi: 10.1158/0008-5472.can-15-1684
52. Krishnamurthy, S., & Basu, A. (2011). Regulation of IKK $\epsilon$  Expression by Akt2 Isoform. *Genes & cancer*, 2(11), 1044–1050. [doi.org/10.1177/1947601912444604](https://doi.org/10.1177/1947601912444604)
53. Guo, J.-P., Tian, W., Shu, S., Xin, Y., Shou, C., & Cheng, J. Q. (2013). I $\kappa$ BKE Phosphorylation and Inhibition of FOXO3a: A Mechanism of I $\kappa$ BKE Oncogenic Function. *PLoS ONE*, 8(5). doi: 10.1371/journal.pone.0063636
54. Boopathy, G. T. K., & Hong, W. (2019). Role of Hippo Pathway-YAP/TAZ Signaling in Angiogenesis. *Frontiers in Cell and Developmental Biology*, 7. doi: 10.3389/fcell.2019.00049
55. Bae, S. J., & Luo, X. (2018). Activation mechanisms of the Hippo kinase signaling cascade. *Bioscience Reports*, 38(4). doi: 10.1042/bsr20171469
56. Gao, Y., Yang, Y., Yuan, F., Huang, J., Xu, W., Mao, B., ... Bi, W. (2017). TNF $\alpha$ -YAP/p65-HK2 axis mediates breast cancer cell migration. *Oncogenesis*, 6(9). doi: 10.1038/oncsis.2017.83
57. Lu, J., Yang, Y., Guo, G., Liu, Y., Zhang, Z., Dong, S., ... Huang, Q. (2017). I $\kappa$ BKE regulates cell proliferation and epithelial-mesenchymal transition of human malignant glioma via the Hippo pathway. *Oncotarget*, 8(30), 49502–49514. doi: 10.18632/oncotarget.17738
58. Liu, Y., Lu, J., Zhang, Z., Zhu, L., Dong, S., Guo, G., ... Huang, Q. (2017). Amlexanox, a selective inhibitor of I $\kappa$ BKE, generates anti-tumoral effects by disrupting the Hippo pathway in human glioblastoma cell lines. *Cell Death & Disease*, 8(8). doi: 10.1038/cddis.2017.396

59. Williams, V., Grosset, A.-A., Cuervo, N. Z., St-Pierre, Y., Sylvestre, M.-P., Gaboury, L., & Grandvaux, N. (2017). Detection of IKK $\epsilon$  by immunohistochemistry in primary breast cancer: association with EGFR expression and absence of lymph node metastasis. *BMC Cancer*, 17(1). doi: 10.1186/s12885-017-3321-6
60. Guadamillas, M. C., Cerezo, A., & Pozo, M. A. (2011). Overcoming anoikis - pathways to anchorage-independent growth in cancer. *Journal of Cell Science*, 124(19), 3189-3197. doi:10.1242/jcs.072165
61. Mori, S., Chang, J. T., Andrechek, E. R., Matsumura, N., Baba, T., Yao, G., . . . Nevins, J. R. (2009). Anchorage-independent cell growth signature identifies tumors with metastatic potential. *Oncogene*, 28(31), 2796-2805. doi:10.1038/onc.2009.139
62. Walsh, N., Clynes, M., Crown, J., & O'donovan, N. (2009). Alterations in integrin expression modulates invasion of pancreatic cancer cells. *Journal of Experimental & Clinical Cancer Research*, 28(1). doi:10.1186/1756-9966-28-140
63. Lin, X., Liu, M., Liu, Y., Hu, H., Pan, Y., Zou, W., . . . Hu, X. (2017). Transforming growth factor  $\beta$ 1 promotes migration and invasion in HepG2 cells: Epithelial-to-mesenchymal transition via JAK/STAT3 signaling. *International Journal of Molecular Medicine*. doi:10.3892/ijmm.2017.3228
64. Huang, P., Xu, X., Wang, L., Zhu, B., Wang, X., & Xia, J. (2013). The role of EGF-EGFR signalling pathway in hepatocellular carcinoma inflammatory microenvironment. *Journal of Cellular and Molecular Medicine*, 18(2), 218-230. doi:10.1111/jcmm.12153
65. Gauthier, A., & Ho, M. (2012). Role of sorafenib in the treatment of advanced hepatocellular carcinoma: An update. *Hepatology Research*, 43(2), 147-154. doi:10.1111/j.1872-034x.2012.01113.x
66. Zhang, L., Zhou, F., & Dijke, P. T. (2013). Signaling interplay between transforming growth factor- $\beta$  receptor and PI3K/AKT pathways in cancer. *Trends in Biochemical Sciences*, 38(12), 612-620. doi:10.1016/j.tibs.2013.10.001
67. Yang, N., Morrison, C. D., Liu, P., Miecznikowski, J., Bshara, W., Han, S., . . . Zhang, J. (2012). TAZ induces growth factor-independent proliferation through activation of EGFR ligand amphiregulin. *Cell Cycle*, 11(15), 2922-2930. doi:10.4161/cc.21386

68. Zhao, Y., Chen, Y., Hu, Y., Wang, J., Xie, X., He, G., . . . Zhang, H. (2018). Genomic alterations across six hepatocellular carcinoma cell lines by panel-based sequencing. *Translational Cancer Research*, 7(2), 231-239. doi:10.21037/tcr.2018.02.14
69. Ezzoukhry, Z., Louandre, C., Trécherel, E., Godin, C., Chauffert, B., Dupont, S., . . . Galniche, A. (2012). EGFR activation is a potential determinant of primary resistance of hepatocellular carcinoma cells to sorafenib. *International Journal of Cancer*, 131(12), 2961-2969. doi:10.1002/ijc.27604
70. Dzieran, J., Fabian, J., Feng, T., Coulouarn, C., Ilkavets, I., Kyselova, A., . . . Meindl-Beinker, N. M. (2013). Comparative Analysis of TGF- $\beta$ /Smad Signaling Dependent Cytostasis in Human Hepatocellular Carcinoma Cell Lines. *PLoS ONE*, 8(8). doi:10.1371/journal.pone.0072252
71. Boyacıoğlu, Z. (2018). ELUCIDATION of SORAFENIB RESISTANCE MECHANISMS IN HEPATOCELLULAR CARCINOMA (Unpublished master's thesis). Bilkent University.
72. Tsai, J. H., & Yang, J. (2013). Epithelial-mesenchymal plasticity in carcinoma metastasis. *Genes & Development*, 27(20), 2192-2206. doi:10.1101/gad.225334.113
73. Muller, V. (2005). Circulating Tumor Cells in Breast Cancer: Correlation to Bone Marrow Micrometastases, Heterogeneous Response to Systemic Therapy and Low Proliferative Activity. *Clinical Cancer Research*, 11(10), 3678-3685. doi:10.1158/1078-0432.ccr-04-2469
74. Evdokimova, V., Tognon, C., Ng, T., & Sorensen, P. H. (2009). Reduced proliferation and enhanced migration: Two sides of the same coin? Molecular mechanisms of metastatic progression by YB-1. *Cell Cycle*, 8(18), 2901-2906. doi:10.4161/cc.8.18.9537
75. Shin, S., Buel, G. R., Nagiec, M. J., Han, M., Roux, P. P., Blenis, J., & Yoon, S. (2019). ERK2 regulates epithelial-to-mesenchymal plasticity through DOCK10-dependent Rac1/FoxO1 activation. *Proceedings of the National Academy of Sciences*, 116(8), 2967-2976. doi:10.1073/pnas.1811923116
76. Salt, M. B., Bandyopadhyay, S., & McCormick, F. (2013). Epithelial-to-Mesenchymal Transition Rewires the Molecular Path to PI3K-Dependent Proliferation. *Cancer Discovery*, 4(2), 186-199. doi:10.1158/2159-8290.cd-13-0520

77. Thomas, L. W., Esposito, C., Stephen, J. M., Costa, A. S., Frezza, C., Blacker, T. S., . . . Ashcroft, M. (2019). CHCHD4 regulates tumour proliferation and EMT-related phenotypes, through respiratory chain-mediated metabolism. *Cancer & Metabolism*, 7(1). doi:10.1186/s40170-019-0200-4
78. Marti, P., Stein, C., Blumer, T., Abraham, Y., Dill, M. T., Pikiolk, M., . . . Tchorz, J. S. (2015). YAP promotes proliferation, chemoresistance, and angiogenesis in human cholangiocarcinoma through TEAD transcription factors. *Hepatology*, 62(5), 1497-1510. doi:10.1002/hep.27992
79. Benyon, B. (2019). FDA approves ramucirumab for hepatocellular carcinoma. *Case Medical Research*. doi:10.31525/cmr-14804cd
80. Center for Drug Evaluation and Research. (2020). FDA grants accelerated approval to nivolumab and ipilimumab combinatio. Retrieved June 30, 2020, from <https://www.fda.gov/drugs/resources-information-approved-drugs/fda-grants-accelerated-approval-nivolumab-and-ipilimumab-combination-hepatocellular-carcinoma>

## Copyright Permissions

### SPRINGER NATURE LICENSE TERMS AND CONDITIONS

Jul 02, 2020

---

---

This Agreement between Bilkent University -- Erta Xhafa ("You") and Springer Nature ("Springer Nature") consists of your license details and the terms and conditions provided by Springer Nature and Copyright Clearance Center.

License Number	4837300151709
License date	May 27, 2020
Licensed Content Publisher	Springer Nature
Licensed Content Publication	Nature Reviews Disease Primers
Licensed Content Title	Hepatocellular carcinoma
Licensed Content Author	Josep M. Llovet et al
Licensed Content Date	Apr 14, 2016
Type of Use	Thesis/Dissertation
Requestor type	academic/university or research institute
Format	electronic
Portion	figures/tables/illustrations
Number of figures/tables/illustrations	1
High-res required	no
Will you be translating?	no
Circulation/distribution	1 - 29
Author of this Springer Nature content	no
Title	MSc.
Institution name	Bilkent University
Expected presentation date	Jun 2020
Portions	Figure 4 Bilkent University 79. lojman merkez campus, bilkent univer
Requestor Location	Ankara, No Selection 06800 Turkey Attn: Bilkent University
Total	0.00 USD

JOHN WILEY AND SONS LICENSE  
TERMS AND CONDITIONS  
Jul 02, 2020

---

---

This Agreement between Bilkent University -- Erta Xhafa ("You") and John Wiley and Sons ("John Wiley and Sons") consists of your license details and the terms and conditions provided by John Wiley and Sons and Copyright Clearance Center.

License Number	4837290435130
License date	May 27, 2020
Licensed Content Publisher	John Wiley and Sons
Licensed Content Publication	CA: Cancer Journal for Clinicians
Licensed Content Title	Global cancer statistics 2018: GLOBOCAN estimates of incidence and mortality worldwide for 36 cancers in 185 countries
Licensed Content Author	Ahmedin Jemal, Lindsey A. Torre, Rebecca L. Siegel, et al
Licensed Content Date	Sep 12, 2018
Licensed Content Volume	68
Licensed Content Issue	6
Licensed Content Pages	31
Type of use	Dissertation/Thesis
Requestor type	University/Academic
Format	Electronic
Portion	Figure/table
Number of figures/tables	1
Will you be translating?	No
Title	MSc.
Institution name	Bilkent University
Expected presentation date	Jun 2020
Portions	Figure 4A Bilkent University 79. lojman merkez campus, bilkent univer
Requestor Location	Ankara, No Selection 06800 Turkey Attn: Bilkent University
Publisher Tax ID	EU826007151
Total	0.00 USD